



HAL
open science

Quantum computers, quantum computing, and quantum thermodynamics

Fabrizio Cleri

► **To cite this version:**

Fabrizio Cleri. Quantum computers, quantum computing, and quantum thermodynamics. *Frontiers in Quantum Science and Technology*, 2024, 3, 10.3389/frqst.2024.1422257 . hal-04683476

HAL Id: hal-04683476

<https://hal.science/hal-04683476v1>

Submitted on 2 Sep 2024

HAL is a multi-disciplinary open access archive for the deposit and dissemination of scientific research documents, whether they are published or not. The documents may come from teaching and research institutions in France or abroad, or from public or private research centers.

L'archive ouverte pluridisciplinaire **HAL**, est destinée au dépôt et à la diffusion de documents scientifiques de niveau recherche, publiés ou non, émanant des établissements d'enseignement et de recherche français ou étrangers, des laboratoires publics ou privés.

Quantum Computers, Quantum Computing and Quantum Thermodynamics

Fabrizio Cleri^{1,2*}

¹*Institute of Electronics, Microelectronics and Nanotechnology (IEMN CNRS UMR8520) Av. Poincaré, Villeneuve d'Ascq, 59652, France*

²*Département de Physique, Université de Lille, Villeneuve d'Ascq, 59650, France*

Correspondence*:

On temporary leave at: LIMMS CNRS IRL2820, University of Tokyo, 4-6-1 Komaba, Meguro-Ku, Tokyo 153-8505, Japan
fabrizio.cleri@univ-lille.fr

2 ABSTRACT

3 Quantum thermodynamics aims at extending standard thermodynamics and non-equilibrium
4 statistical physics to systems with sizes well below the thermodynamic limit. A rapidly evolving
5 research field, which promises to change our understanding of the foundations of physics, while
6 enabling the discovery of novel thermodynamic techniques and applications at the nanoscale.
7 Thermal management has turned into a major obstacle in pushing the limits of conventional
8 digital computers, and could likely represent a crucial issue also for quantum computers. The
9 practical realization of quantum computers with superconducting loops requires working at
10 cryogenic temperatures to eliminate thermal noise; ion-trap qubits need as well low temperatures
11 to minimize collisional noise; in both cases, the sub-nanometric sizes also bring about thermal
12 broadening of the quantum states; and even room-temperature photonic computers require
13 cryogenic detectors. A number of thermal and thermodynamic questions therefore take center
14 stage, such as quantum re-definitions of work and heat, thermalization and randomization of
15 quantum states, the overlap of quantum and thermal fluctuations, and many other, even including
16 a proper definition of temperature for the small open systems constantly out of equilibrium that
17 are the qubits. This overview provides an introductory perspective on a selection of current trends
18 in quantum thermodynamics and their impact on quantum computers and quantum computing,
19 with a language accessible also to postgraduate students and researchers from different fields.

20 **Keywords:** thermodynamics, qubits, quantum gates, information entropy, thermalization

1 INTRODUCTION

21 Quantum computing has gone a long way, from the dream of Richard Feynman expressed in his keynote
22 paper of 1982 (Feynman (1982)), to the increasingly sophisticated theoretical developments that followed
23 in the '90s, to the first realizations of experimental quantum bits in the past 20 years (Editorial (2022);
24 Huang et al. (2020); Pelucchi et al. (2022)). Today we are just starting to see the first true quantum
25 machines sporting some tens of qubits connected by fully reversible quantum gates, which attempt at
26 solving theoretical benchmark challenges. It is not still the calculation of real-life problems, however they
27 are getting a bit closer every few months, in a path that seems to echo the spectacular growth of digital
28 microelectronics in the last half of the past century.

29 By looking at the latest developments among the main players in quantum hardware and software,
30 Google's Quantum-AI subsidiary Alphabet first reported having reached "quantum advantage" in July 2019
31 with their Sycamore machine (Arute et al. (2019)), a claim later challenged by IBM engineers. (see below)
32 Both IBM and Google use qubits made with superconducting loops. IBM broke already the 100-wall with
33 its 127-qubit Quantum Eagle (Kim et al. (2023a)), and just announced its new milestone by the end of 2023
34 with his QuantumSystem-Two modular architecture including three Heron 133-qubit devices. Also Intel
35 is engaged in both superconducting and spin qubit research: June 2023 unveiled its new TunnelFalls, a
36 12-qubit all-silicon chip. NVIDIA launched in March 2023 the DGX Quantum, a GPU-accelerated system,
37 integrating their GraceHopper superchip with the OPX platform by Quantum Machines. Honeywell opted
38 for trapped-ion qubits in their System-Model H1, 10-qubit first operational machine, already used for
39 quantum chemistry simulations (Yamamoto et al. (2024)); a similar road to that followed by IonQ with their
40 Aria 25-qubit machine. **Microsoft chose to work with a different concept for their Azure quantum system,
41 the "topological" qubits (Aghaee et al. (2023)), for which they received DARPA support; however, they
42 also pursue a different, hybrid strategy by coupling qubit-virtualization with ion-trap physical qubits from
43 Quantinuum, to achieve extremely low error rates (da Silva et al. (2024)).** Notably, all these companies are
44 making their computing platforms, or a scaled-down version thereof, publicly web-accessible to anybody
45 for testing and running quantum codes via the internet. In June 2022, the US Senate passed the \$250
46 billion Innovation and Competition Act, promoting quantum information technologies among the actions to
47 ensure that the US semiconductor and information technology continue to play a leading role in the global
48 economy. At the other shore of the Pacific, with the help of a multi-billion-dollar funding package and a
49 €10 billion investment in a quantum information laboratory, China hopes to make significant breakthroughs
50 in the field by 2030. Big names such as Alibaba and Baidu are engaged in sustaining R&D (although
51 Alibaba's quantum laboratory was suddenly shut down Nov. 2023). But already, one team at the University
52 of Science and Technology of China in Hefei, reported achieving quantum advantage by using two radically
53 different technologies, linear optics or superconducting qubits, just one year apart from each other (Wu
54 et al. (2021); Zhong et al. (2021)).

55 As far as Europe, In October 2018 the European Commission launched the "Quantum Technologies
56 Flagship" programme, to support hundreds of quantum science researchers over a ten-year period with a
57 budget of €1 billion. The OpenSuperQPlus project is a medium-term, 4-year project centered at the Jülich
58 Research Center in Germany, assembling 28 partners from 10 EU countries. However, compared to the US
59 and China market dominated by a few hi-tech giants, the EU panorama is richer in smaller partnerships and
60 smaller companies (Räsänen et al. (2021)). UK, sadly no longer part of the European Union, has announced
61 conspicuous investments, while initially relying on technology provided by the US start-up Rigetti, and
62 other local solutions such as the OQC company in Oxford developing their "coaxmon" (Rahamim et al.
63 (2017)). As usual, other EU countries are proceeding working the two sides of the street, partly following
64 EU guidelines and partly pushing national initiatives. Germany follows a strategy similar to UK, coupling
65 €3 billion in national investment with US quantum technology imported from IBM. Netherlands launched
66 its national quantum strategy in 2019 with €615 million and the Quantum Delta NL initiative to help
67 quantum research and marketing in universities. France follows, as it often happens, a more original way,
68 with a 5-year €1.8 billion funding initiative (half of which coming from public money), the development of
69 a large-scale quantum annealer (a somewhat different concept from the gate-based quantum computer) by
70 the start-up company Pasqal (Schymik et al. (2022)), and in parallel the Quandelà (Somaschi et al. (2024))
71 just-announced photonic computer installed in the north of France.

72 Then, why thermodynamics? Heat dissipation has always been a crucial problem for digital computers,
73 and represents probably the biggest limit to a further expansion of the CMOS-based computing technology
74 (Kish (2002); Valavala et al. (2018); Bespalov et al. (2022)). Up to the '90s, the solution was to reduce the
75 voltage levels, but now we are already at 0.7 V and this figure could not be reduced further. The heating
76 problem has been exacerbated with the introduction of 3-dimensional design, that brought with it new issues
77 of capacitive charging of the metal connections crossing in the vertical direction. The progressively reduced
78 transistor dimension, now at limits reaching below the 10 nm, has the additional issue of self-heating
79 because of the largely increased surface/volume ratio of the device. Switching is also at its limits: we have
80 devices in our laboratories that can easily function at 100 GHz and more, however the fastest clock cycle
81 adopted in real computing units cannot go above the 5-6 GHz, just because the rate of heat accumulation
82 cannot be matched by a fast-enough rate of dissipation. Quantum computers could be in principle even
83 more sensitive to fluctuations and heat dissipation, since qubits are designed at the quantum scale, and the
84 thermal energy can represent a source of noise (interference) in their wavefunction. Discrete energy spectra
85 are typically very sensitive to small perturbations that can break symmetry-related degeneracies. Notably,
86 in order to prepare (reset) and retrieve the information of a qubit its quantum state must be destroyed, an
87 operation that necessarily entails some heat release. Until now, such a problematic (a.k.a. ensemble of
88 connected problems) has received a comparatively little attention, because of the already outstanding issues
89 represented by noise from imperfect control signals, interference from the environment and unwanted
90 interactions between qubits, the need for quantum error correction, and the need for operating at cryogenic
91 temperatures. However, questions about temperature, entropy, work, heat, take a very peculiar angle, when
92 seen in the context of quantum mechanics and notably of quantum computing.

93 The purpose of this article¹, halfway between a review and a primer, is to give a concise summary of the
94 emerging field of quantum thermodynamics in relation to quantum computing. I should maybe provide a
95 more precise definition at the outset, since it may appear an oxymoron to put together in the same sentence
96 the word "thermodynamics", that is the phenomenological theory of the average macroscopic behavior of
97 heat and work exchanges, and the word "quantum", that in itself represents the epitome of the microscopic
98 world. The two major shortcomings when trying to apply thermodynamics to the quantum domain should
99 be (1) the fact that, by its proper definition, thermodynamics does not contain microscopic information, nor
100 does it have a protocol to relate to the microscopic degrees of freedom; and (2) the fact that it describes only
101 equilibrium states. The first one can be circumvented by passing to the statistical mechanics formulation of
102 thermodynamics, which provides the proper equations and language to make the link with the microscopic.
103 The solution to the second one can leverage on the developments of stochastic thermodynamics, which uses
104 stochastic variables (thus offering a link with the quantum-mechanical notion of probability) to describe
105 the non-equilibrium dynamics typically observed at the molecular length and time scales.

106 Quite obviously, quantum thermodynamics covers more general questions than just quantum information.
107 Machines that convert heat into electrical power at a microscopic level, where quantum mechanics plays a
108 crucial role, such as thermoelectric and photovoltaic devices, are well known examples of systems requiring
109 the new language of quantum thermodynamics. It is often said that such machines differ from conventional
110 machines by having no moving parts; however, while they may have no *macroscopic* moving parts, they
111 function with steady-state currents of microscopic particles (electrons, photons, phonons, etc.) which
112 are all quantum in nature. Nanotechnology has significantly advanced efforts in this direction, offering
113 unprecedented control of individual quantum particles. The questions of how this control can be used for

¹ An extended and updated version of a series of lectures given between January and April 2022, at the Quantum Information Working Group in the University of Lille, France.

114 new forms of heat-to-work conversion has started to be addressed in recent years (Benenti et al. (2017);
115 Bhattacharjee and Dutta (2021)).

116 Hence, our title starts from quantum computers and moves to quantum computing, stressing the fact that
117 to realize a quantum computation you first need to build a physical quantum machine. (Not so obvious,
118 because one can also try to simulate the quantum computation on a classical computer.) The role of
119 thermodynamics, and notably of entropy, therefore will play a dual role in this context, in that it affects
120 both the physical system *and* the computation that is being carried out on that system. Entropy will have a
121 special position, since its different definitions seem to start from rather different premises each time, but
122 eventually end up to very similar, if not formally identical, formulations. We will ask whether a formal
123 similarity also implies, and to what extent, physical identification between different definitions.

124 This contribution is organized as follows: Sections 2 and 3 give a rapid overview (necessarily incomplete
125 and partial, given the obvious limitations of space) of quantum computers and quantum computing,
126 just some basic details to make this article self-contained for the materials that follow; I will mainly
127 focus as a representative example on superconducting loops and the TransMon that, at this stage of
128 development, seemingly represent the most popular choice of constructors; Section 4 recalls some notions
129 of basic thermodynamics in the context of digital computers; Section 5 deals with the link between
130 thermodynamic entropy and information entropy, and the (ir)reversibility of quantum computations;
131 Section 6 is both the longest and the richest of possibly novel ideas, discussing the reformulation of
132 some classical thermodynamics concepts in the framework of quantum mechanics, and providing several
133 examples of key questions in which quantum thermodynamics can make an impact on quantum computing.
134 Some conclusions and outlook are given in the final Section 7.

2 ON THE ADVANTAGE OF QUANTUM COMPUTING

135 Quantum advantage (the old word to indicate the computational gain of a quantum device compared to a
136 classical digital computer was "supremacy", but it is currently replaced by "advantage", or "computational
137 advantage") typically refers to situations in which information processing devices built on the principles of
138 quantum physics, attempt at solving computational problems that are not tractable by classical computers.
139 The resulting quantum advantage is usually defined as the ratio of classical resources required to solve the
140 problem, such as time or memory, to the associated quantum resources. Notably, the numerator in this ratio
141 is often just an estimation, since the problems that are faced are by definition beyond the reach, or at the
142 limits of the capabilities of classical digital computers. Quantum thermodynamics will offer an interesting
143 additional perspective, by comparing also energy dissipation between classical and quantum computing.

144 Maybe some points need to be clarified, to start with. A quantum computer can use bits and logic gates,
145 just as a digital computer does, therefore at least in theory it should be able to do any computation a classical
146 computer can do, plus a number of other computations that are beyond classical. From the standpoint
147 of computability theory, the key difference between the two is in the state of the bits at any stage of the
148 computation: a classical bit is always in either one of two defined states; a quantum bit is always in a
149 combined state overlapping with the states of (some or all) the other bits. In this way, the interference
150 among quantum bits creates stronger correlations than allowed by classical probability rules (Rau (2009);
151 Wilce (2021)), and can force some bit combinations to be more likely than others.

152 Measuring a quantum state implemented on a quantum computer, however, will return only classical
153 information, that is, strings of binary code. Then, how can we be sure that a quantum computation was
154 carried out, and not a classical one? Well, the first and simplest check would be to execute many times the

155 same computation. Since quantum computers operate on probabilistic principles, the answer should not be
156 unique but rather a distribution of occurrences, with one being (hopefully) the most probable. Any simple
157 quantum operation, such as summing two bits, necessarily gives a probabilistic answer. See for example
158 the original quantum full adder (Feynman (1985)) and its optimized versions (Maslov et al. (2008)): even
159 the best implementation gives a fidelity of 83.333% (Figgatt et al. (2019)). So, in this case the constant
160 and deterministically repeatable answer of the classical computer is definitely preferable. A recent work
161 (Tindall et al. (2024)) proved that, by a judicious restructuring of the classical algorithm, even a laptop can
162 outperform the noisy results of the quantum computer on a problem for which an exact solution can be
163 calculated as reference, such as the short-time evolution of the 2D-Ising model.

164 Therefore, the real challenge would be to propose to the quantum computer a problem that is known to
165 be unsolvable for the classical computer. Beware of the fact that here we intend a class of problems, not a
166 particular instance of the class. "Factorization" is a class of problems, "factorizing the number 4321" is an
167 instance: a classical or quantum algorithm could be good at solving a particular instance, but we are better
168 interested in algorithms that solve the entire class.

169 In computation theory, problems whose solution can be obtained in a time that is some power of the
170 size (that is, resources, number of bits, energy) are called polynomial, or P. Given enough resources, a
171 classical computer like a Turing machine can solve any of these P-problems. By contrast, problems that
172 in the general case cannot be solved in a time that grows at best polynomially with the size, are called
173 NP (yes, we are dividing the world into elephants and non-elephants). Factorization of integer numbers
174 is the most typical problem of this kind. A classical computer cannot decompose into prime numbers an
175 integer of arbitrary size, since it would run out of resources at a rate faster than the growth of the required
176 integer. (The largest number factorized, RSA-250 with 795 bits, took the equivalent of 2,700 years on a big
177 supercomputer (Boudot et al. (2020)).)

178 Already 30 years ago, Peter Shor proposed a quantum-mechanical algorithm that reduces to P-class the
179 NP complexity of factorization, if implemented on an ideal quantum computer (Shor (2004, 2007)). Since
180 then, his algorithm has been programmed on a few different quantum computers, e.g. to factor the number
181 15 already several times, and more recently the number 21 by using an iterative algorithm to limit the
182 number of necessary qubits (Martín-López et al. (2012)). In fact, Shor's algorithm to factor an odd integer
183 N requires a work register with $\log_2 N$ qubits, plus an output register with m qubits for a precision of m
184 digits: the result will appear as a series of probability peaks in the output register, the narrower and higher,
185 the larger is m . The total of resources required is not impressive, but quantum computers with more than a
186 few qubits are still difficult to build, one big problem being the growth of the error rate with the number of
187 entangled qubits. The most recent attempt at factorizing the number 35 on the IBM Q-System-One failed
188 just because of error accumulation (Amico et al. (2019)).

189 Next to problems of deterministic complexity (P, NP, NP-hard, NP-complete), a class of bounded-error
190 probabilistic-polynomial problems, or BPP, has been defined. These are problems that can be solved in
191 a polynomial time and include random processes (such as in a probabilistic Turing machine), but are
192 bounded, meaning that the algorithm gives the right answer with a large probability, fixed at $2/3$. Obviously,
193 problems that are in the P class are also in the BPP class, and it is believed (but not proven) that the two
194 classes coincide, especially after it was demonstrated that the primality problem (i.e., determining whether
195 a number is prime) is also in P (Agrawal et al. (2004)).

196 By lowering the requirement of giving the correct answer to more than $1/2$ probability (that seems just
197 one inch above the tossing of a coin to find the answer), the larger class of PP (probabilistic-polynomial)

198 problems is defined. And somewhere between the two, there is the BQP class, or bounded-error quantum-
199 polynomial complexity (Bernstein and Vazirani (1997)). By definition, BQP contains all BPP problems,
200 and obviously all P problems; it also includes some NP problems, such as factorization. And it includes
201 some problems "beyond-NP", that is, problems for which a classical computer cannot find, or even check
202 the correctness of, the answer in a polynomial time. An example is the boson sampling problem, in which
203 somebody wants to determine the probability distribution of an ensemble of M identical, non-interacting
204 bosons (photons, spin-0 atoms²) after scattering through an interferometer. Aaronson and Arkhipov (2011)
205 Such a physical experiment requires a mathematical tool to calculate the answer, the *permanent* of an
206 $M \times M$ matrix, which would normally require an exponential time to compute ($\mathcal{O}(M^2 2^M)$) on a classical
207 computer (Marcus and Minc (1965)). Therefore, this seems like an ideal case in which to test the advantage
208 or "supremacy" of a quantum computer with respect to classical, digital computers (see below).

209 **What do quantum computers look like, A.D. 2024?** The hardware requirements to achieve computational
210 advantage can be summarized by three key properties:

- 211 • the quantum systems must initially be prepared in a well-defined pure state;
- 212 • arbitrary unitary operators must be available and controllable in order to launch an arbitrary entangled
213 state;
- 214 • measurements (read-out) of the qubits must be performed with high quantum efficiency.

215 We can rank the different solutions proposed up to date in about three broad classes:

216 *Gate-based quantum computation* and the related class of universal digital algorithms, are approaches
217 that rely on a quantum processor, encompassing a set of interconnected qubits, to solve a computation that
218 is not necessarily quantum in nature. The dominant technique for implementing single-qubit operations is
219 via microwave irradiation of a superconducting loop (see below, Sect.3). Circuit quantum electrodynamics
220 (CQED), the study and control of light-matter interaction at the quantum level (Blais et al. (2021)),
221 plays an essential role in all current approaches to gate-based digital quantum information processing
222 with superconducting circuits. Electromagnetic coupling to the qubit with microwave pulses at the qubit
223 transition frequency drives Rabi oscillations in the qubit state; control of the phase and amplitude of
224 the drive is then used, to implement rotations about an arbitrary axis of the quantum state of each qubit;
225 these are the logical gates, which perform the sequence of required operations in the algorithm as a
226 sequence of unitary transformations of the state of the ensemble of qubits. Typically, current universal
227 algorithms are tailored to a specific, and potentially noisy hardware (noisy intermediate-scale quantum-, or
228 NISQ-technology (Cheng et al. (2023); Kim et al. (2023b))) in order to maximize the overall fidelity of the
229 computation, despite the absence of a yet complete and reliable scheme for quantum error correction. (See
230 for example the reviews in Kjaergaard et al. (2020); Huang et al. (2020). More on this class of devices in
231 the following.)

232 *Adiabatic quantum computation* is an approach formally equivalent to universal quantum computation,
233 in which the solution to computational problems is encoded into the ground state of a time-dependent
234 Hamiltonian. Solving the problem translates into an adiabatic (that is, very slow) quantum evolution towards
235 the global minimum of a total-energy landscape that represents the problem Hamiltonian. Compared to
236 numerical annealing on a classical computer, achieved by using simulated thermal fluctuations to allow

² In these experiments, atoms such as ⁸⁷Rb or ¹³³Cs are used, which do not look like bosons. At low temperatures, however, electrons and the nucleus behave as a unique ensemble, so that the Rb spin-3/2 nucleus plus the 37 spin-1/2 electrons make up a single system with integer spin.

237 the system to escape local minima (such as in the kinetic Monte Carlo method), in quantum annealing the
238 transitions between states are caused by quantum fluctuations, rather than thermal fluctuations, leading to a
239 highly efficient convergence to the ground state for certain problems. The D-WAVE quantum annealers are
240 a successful line of development of this scheme, having already demonstrated the successful operation of
241 a machine with more than 2,000 superconducting flux qubits, on real physics problems (see e.g. Harris
242 et al. (2018)). More generally, any optimization problems that can be reframed as minimization of a cost
243 function (the "total energy") could be efficiently run on such devices. It may be worth noting that up to
244 now, there is still no firm proof that an adiabatic computer could offer an effective speed-up (advantage)
245 over an equivalent classical computation (Ronnow et al. (2014); Yarkoni et al. (2022)).

246 *Quantum simulators* are well-controllable devices that mimic the dynamics or properties of a complex
247 quantum system that is typically less controllable or accessible. The key idea is to study relevant quantum
248 models by emulating or simulating them with an hardware that itself obeys the laws of quantum mechanics,
249 in order to avoid the exponential scaling of classical computational resources. Quantum simulators are
250 problem-specific devices, and do not meet the requirements of a universal quantum computer. This
251 simplification is reflected in the hardware requirements and may allow for a computational speed-up with
252 few, even noisy quantum elements, for example by emulating specific Hamiltonians and studying their
253 ground state properties, quantum phase transitions, or time dynamics (see e.g. Fitzpatrick et al. (2017);
254 Ma et al. (2019)). Therefore, quantum simulators might be ready to address meaningful computational
255 problems, demonstrating quantum advantage well before universal quantum computation could be a reality.

256 **Chariots of fire.** The first claim of quantum computational advantage was launched in 2019, with the
257 general-purpose Sycamore quantum processor, housing 54 superconducting programmable TransMon
258 qubits operating at 10 mKelvin, built by a team of Google engineers in Santa Barbara, CA (Arute et al.
259 (2019)). The qubits are arranged in a rectangular 9×6 Ising layout, with gates operating either on single
260 qubits, or pairs of neighbor qubits. Pseudo-random quantum circuits are realized by alternating single-qubit
261 and two-qubit gates, in specific, semi-random patterns. This gives a random unitary transformation perfectly
262 compatible with the hardware. The circuit output is measured many times, producing a set of sampled
263 bit-strings. The more qubits there are, and the deeper the circuit is, the more difficult it becomes to simulate
264 and sample these bit-string distributions on a classical computer. By extrapolation, Google engineers
265 estimated that a sampling that required about 200 seconds run on Sycamore would have taken $\sim 10,000$
266 years on a million-core supercomputer. However, the claim was questioned by a team at IBM (whose
267 quantum computer Q-system One is also based on superconducting qubits) who devised a much faster
268 classical algorithm, based on which they predicted (yet without performing it) that the classical calculation
269 would get down to about 2-3 days. Two years later, a Chinese team used a tensor-based simulation on their
270 Sunway digital supercomputer, to perform the same simulation in 304 seconds (Liu et al. (2021)).

271 **The Dragon Labyrinth.** It has been demonstrated already some time ago that by using only linear optical
272 elements (mirrors, beam splitters, phase shifters) any arbitrary 1-qubit unitary operation, or equivalent
273 quantum gate, can be reproduced (Knill et al. (2001)). The flip side of the coin is that photon-based
274 implementation is not a very compact architecture. However, photonic quantum microcircuits are under
275 active development (see the Canadian startup *Xanadu*, Madsen et al. (2022)). The boson random sampling
276 experiment, proposed by Aaronson and Arkhipov at MIT (Aaronson and Arkhipov (2011)), entails
277 calculating the probability distribution of bosons whose quantum waves interfere by randomizing their
278 positions. The probability of detecting a photon at a given position (e.g. behind a diffraction grating)
279 involves practically intractably big matrices (the "Torontonion" requires to compute 2^N determinants of

280 rank N) The Heifei University group published results of their largest optical quantum computer (Zhong
 281 et al. (2021)). They used 72 indistinguishable single-mode Gaussian squeezed states as input, injected
 282 into a 144-mode ultralow-loss interferometer, generating entangled photon states in a Hilbert space of
 283 dimension $2^{144} \simeq 10^{43}$. The classical solution requires calculating 10^{43} determinants 144×144 , so the
 284 “supremacy” in this case is clearly indisputable.

3 SUPERCONDUCTING QUBITS AND QUANTUM GATES

285 A simple search on the internet will present you a fairly large number of options to realize a quantum bit,
 286 or *qubit*, ranging from cold atoms (Wintersperger et al. (2023)), to trapped ions (Bruzewicz et al. (2019)),
 287 to nuclear spins, quantum dots, topological systems with a gap, and others. However, when it comes to
 288 practical implementations on currently existing quantum computers, the long list turns into a rather short
 289 one. Basically, only three choices along with some variants, are the ones found along the beaten path:
 290 superconducting quantum dots, ion traps, and photonic circuits. To avoid excessive length, this article
 291 will not deal with photon-based computing. Aside of the long tradition that makes generation, control
 292 and measurement of photons as quantum systems a routine in many laboratories and industry, and despite
 293 their many advantages, among which working at room temperature, photon-based quantum computing has
 294 one major disadvantage, in that photons do not interact with each other. This key issue requires a special,
 295 dedicated approach to the problem, which is well described in a number of excellent reviews already (see
 296 e.g. Slussarenko and Pryde (2019); Pelucchi et al. (2022); Giordani et al. (2023)). Hence, since this is not
 297 primarily a review on quantum computing hardware, I will briefly discuss in this Section as a practical
 298 example of physical implementation only the superconducting (SC) qubits, which are up to now the most
 299 popular choice (IBM, Google, Rigetti, and others), in its two main variants, the charge and the flux qubit.

300 **TransMon basics.** The basic idea behind the SC qubit is to create a tunable oscillator in the solid-state
 301 with well defined quantum mechanical states, between which the system can be excited by means of an
 302 external driving force. The quantum harmonic oscillator is a resonant circuit that can be schematized as a
 303 typical LC-circuit-equivalent, with characteristic inductance $L \simeq 1$ nH and capacitance $C \simeq 10$ pF, which
 304 result in a resonant frequency:

$$f = \frac{1}{2\pi\sqrt{LC}} \simeq 1.6 \text{ GHz, and } \lambda = \frac{c}{f} \simeq 2 \text{ cm} \quad (1)$$

305 In order to address quantum states individually a non-linear component to the circuit must be introduced,
 306 thus making it an anharmonic circuit. A Josephson junction (J-J) is a device that consists of an insulator
 307 “sandwiched” between two superconductors, and can act as a non-dissipative and non-linear inductance.
 308 For this purpose, temperature must be in the mK range, sufficiently low for electrons to condense below
 309 the Fermi energy and form Cooper pairs.

310 Since the dimensions of the J-J are of only a few hundred μm (i.e., much less than the circuit’s operating
 311 wavelength λ above), everything falls well within the lumped-element limit, and it can be described by
 312 using one collective degree of freedom Φ (the magnetic flux). In its basic implementation, the SC qubit can
 313 be designed in different manners: (1) as a *charge* qubit, composed of a J-J and a capacitor; adjusting the
 314 voltage can control the number of Cooper pairs; (2) as a *flux* qubit, with a loop inductance replacing the

315 capacitor; changing the bias flux can adjust the energy level structure; (3) as a *phase* qubit, with just the J-J
 316 and a current modulator; adjusting the bias current can tilt the potential energy surface.

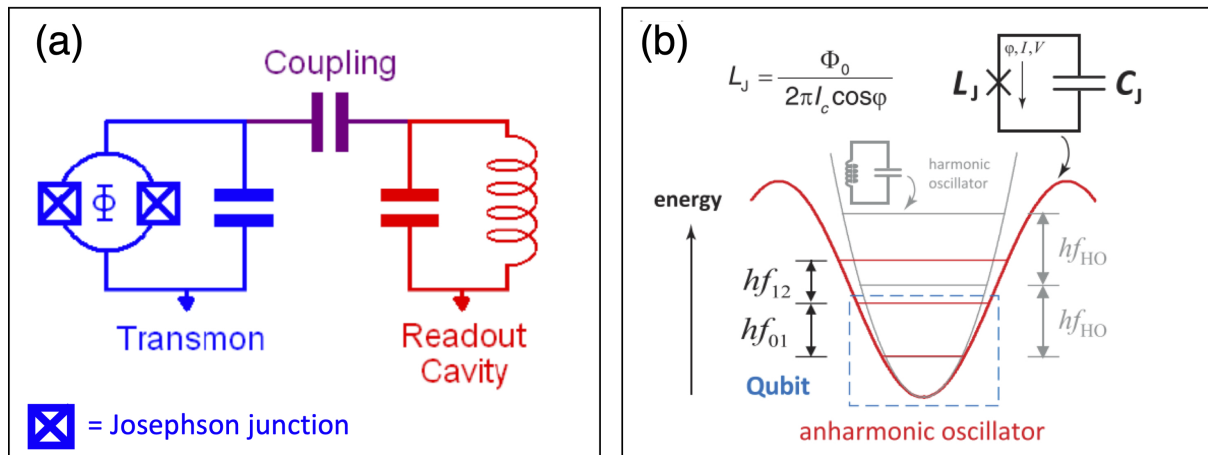


Figure 1. Basic scheme of a Transmon. **(a)** The double J-J forming a loop, with its shunting capacity (blue), the read-out LC resonator (it could be replaced by a resonant cavity), and the coupling capacity (grey). **(b)** Difference between the linearly-spaced levels of the harmonic oscillator, and the non-linearly-spaced levels in the magnetically driven cosine potential.

317 For Φ to be treated as a quantum-mechanical variable, the width of the energy levels of the resonator
 318 must be smaller than their separation, which puts a constraint on the damping Q of the oscillator. Hence, to
 319 keep a $Q \gg 1$, the inductor could only be made by a superconducting wire: a quantum- LC resonator. But a
 320 single quantum- LC is still a harmonic oscillator, which means that its equally-spaced energy levels are not
 321 individually addressable. It is then impossible to restrict the system to only two states, as a qubit requires.

322 However, the magnetic energy in the J-J is not classically quadratic in the flux, but rather proportional to
 323 the cosine of Φ , as $E_J = E_J^{max} |\cos(\pi\Phi/\Phi_0)| = L_J I_c^2$. Here $I_c = 2E_J/\hbar$ is the critical current (maximum
 324 current that can flow coherently through the junction), $\Phi_0 = \hbar/2e$ is the SC quantum, and $L_J = \Phi_0/2\pi I$
 325 is the J-J inductance. The junction current is $I = I_c \sin \phi$, with $\phi = (2\pi/\Phi_0)\Phi$ the Josephson phase (Blais
 326 et al. (2021); Kjaergaard et al. (2020)). Due to this anharmonicity (Fig.1b), the ground and first-excited
 327 states of the Cooper pair may be uniquely addressed at a frequency f_{01} , typically in the microwave range
 328 4-8 GHz, without significantly perturbing higher-excited states of this “artificial atom”. Then, the two
 329 lowest-energy states make up an effective two-level system, i.e. a “pseudo-spin-1/2” system, although the
 330 SC loop *per se* would not be a true 2-level system.

331 **Charge qubit.** Starting from the three basic implementations, different and more advantageous types of SC
 332 qubits have been invented, the TransMon being by far the most popular. Based on the charge-qubit model,
 333 in which the number of Cooper pairs N is the main variable, a flux-tunable transmon can be realized with
 334 double J-J (a modified SQUID loop, first proposed by J. Koch’s group in 2007 (Koch et al. (2007), Fig.1a)
 335 that can store an energy $E_J = (\Phi_0/2\pi)I$. The circuit is shunted by a large coupling capacitance, such that
 336 the coupling energy $E_C = e^2/2C \ll E_J$, thus giving a large Q . The advantage of such a double-J-J is that
 337 the values of magnetic flux Φ can be fine-tuned, and each qubit can be individually addressed by a “gate”
 338 (actually, a sequence of GHz pulses). The state of the qubit is readout by a second resonator (“cavity”)
 339 whose resonant frequency f_R is chosen to be far from f_{01} . Then, the two possible qubit states show up as a
 340 (small) red- or blue-shift Δ about the central readout frequency, $f_R \pm \Delta$.

341 The Hamiltonian of the classical equivalent circuit can be written as:

$$\mathcal{H} = 4E_C \left(N - \frac{1}{2}\right)^2 - E_J \cos \phi + \underline{W(t) \sin(\Omega_R t + \phi)} \quad (2)$$

342 The quantum version for the TransMon qubit (such as found in IBM Quantum System, or Google
343 Sycamore) runs on a slightly modified version of the celebrated Jaynes-Cummings theoretical model (Lo
344 et al. (1998)), and looks like:

$$\hat{\mathcal{H}} = \hbar\sqrt{8E_C E_J} \left(a^\dagger a + \frac{1}{2}\right) - \hbar E_C \left(a\hat{\sigma}^+ + a^\dagger\hat{\sigma}^-\right) + \underline{\Omega_R [\mathcal{J}(t)\hat{\sigma}_x + \mathcal{Q}(t)\hat{\sigma}_y]} \quad (3)$$

345 In the two equations, the underscored parts represent the external field (a train of microwave pulses)
346 driving the Hamiltonian. N is the number of excess Cooper pairs (destroyed/created by the operators
347 $a, a^\dagger = \sqrt{n} |n \mp 1\rangle \langle n \pm 1|$; $\hat{\sigma}_{x,y,z}$ and $\hat{\sigma}^\pm = \hat{\sigma}_x \pm i\hat{\sigma}_y$ are Pauli matrices; Ω_R is the Rabi frequency; \mathcal{J}
348 and \mathcal{Q} are the in-phase and quadrature components of the microwave signal $W(t)$. In principle, N and ϕ
349 are both good quantum numbers to describe the TransMon; however, in the $E_C \ll E_J$ limit only N is well
350 defined, while ϕ fluctuates randomly.

351 **Flux qubit.** A variant of the transmon is realized with a SC ring interrupted by 3 or 4 Josephson junctions.
352 The qubit is engineered so that a persistent current flows continuously when an external magnetic flux is
353 applied. Only an integer number of flux quanta penetrate the SC ring, resulting in clockwise or counter-
354 clockwise mesoscopic supercurrents (typically 300 nA) in the loop, which compensate (screen or enhance)
355 a non-integer external flux bias. The ϕ degree of freedom becomes now the main variable, the number of
356 flux quanta N being random, and the coupling energy dominates over the charging energy, $E_J \ll E_C$.

357 When the applied flux through the loop is close to a half-integer number of flux quanta, the two lowest-
358 energy loop eigenstates are found in a quantum superposition of the two currents. This is what makes the
359 flux qubit a spin-1/2 system, moreover with separately tunable z and x fields,

360 The flux qubit has been used as building block for quantum annealing applications based on the transverse
361 Ising Hamiltonian (Hauke et al. (2020)). A typical quantum Hamiltonian that can be implemented in a
362 connected network of flux qubits, such as in the D-WAVE Chimera or Pegasus architectures, looks like:

$$\hat{\mathcal{H}} = \Lambda(t) \left[\sum_i h_i \hat{\sigma}_i^z + \sum_{i<j} J_{ij} (\hat{\sigma}_i^z \cdot \hat{\sigma}_j^z) \right] + \Gamma(t) \sum_i \Delta_i \hat{\sigma}_i^x \quad (4)$$

363 The h_i are asymmetry energies, J_{ij} represent the coupling matrix elements, and Δ_i are tunneling energies.

364 At the beginning of the quantum annealing process, it is $\Gamma(0)=1$ and $\Lambda(0)=0$, to create a known ground
365 state as an equal superposition in the computational basis. During the adiabatic annealing protocol, the two
366 parameters slowly evolve towards $\Gamma \rightarrow 0$ and $\Lambda \rightarrow 1$.

367 Other transmon variants have been proposed to counter some of the practical problems encountered in
368 the different SC loops implementations, such as the C-shunt flux qubit (You et al. (2007)), to reduce charge
369 noise; the "fluxonium" (Manucharyan et al. (2009)), to address the noise from inductance and offset charge;

370 the "0- π " qubit (Brooks et al. (2013); Gyenis et al. (2021)), designed to improve the symmetry of the two
 371 current states; and various types of hybrid qubits (see, e.g., Marcos et al. (2010); Kubo et al. (2010); Zhu
 372 et al. (2011)), in which the SC loops are coupled to solid-state elements, a doped crystal, or a resonant
 373 cavity, to exploit the advantages from different quantum effects. Over the recent years, the key objective
 374 of increasing the lifetime of the qubit state has been pursued, extending the coherence time from mere
 375 fractions of μs well into the ms domain (Pop et al. (2014)).

376 The next important operation to consider is the read-out of the information from the qubit. **For solid-state**
 377 **qubits, this may be performed by energy-selective escape from a metastable potential (Martinis et al. (2002);**
 378 **Hanson et al. (2005)), or with a bifurcation amplifier (Siddiqi et al. (2004); Mallet et al. (2009)).** For the
 379 SC loops, it is possible to detect either charge, flux, or inductance. A popular method is the dispersive
 380 read-out (Wallraff et al. (2004)), in which the qubit and the resonator (see again Fig.1a) are coupled by a
 381 strength parameter $g \ll \Delta = \omega_{01} - \omega_R$, as in the approximate Hamiltonian:

$$\hat{\mathcal{H}} = -\frac{\omega_{01}}{2}\hat{\sigma}^z + \left(\omega_R + \frac{g^2}{\Delta}\hat{\sigma}^z\right)a^\dagger a \quad (5)$$

382 The presence of a $|0\rangle$ or $|1\rangle$ state in the qubit shows up as a small frequency shift in the resonator by the
 383 quantity g^2/Δ . The read-out is "dispersive" in the sense that the signal corresponding to the two possible
 384 states appears clustered in two disjointed clouds in the complex plane (Blais et al. (2021)). **The theory**
 385 **behind this technique has been established for systems both in and out-of equilibrium, for general two-level**
 386 **driven systems, non-Markovian dynamics, and thermally excited multilevel systems (Kohler (2017, 2018);**
 387 **Shen et al. (2022); Yang and Shen (2024)).**

388 **Qubits and quantum gates.** Independently on their actual physical implementation, qubits are
 389 mathematically defined as two-state quantum systems, described by a state vector in a 2-dimensional
 390 Hilbert space, spanning a closed surface with conserved norm (i.e., a sphere, called the "Bloch sphere",
 391 Figure 2a). A standard basis is defined by the two vectors $|0\rangle$ and $|1\rangle$, conventionally aligned with the
 392 positive and negative direction of the z-axis.

393 A quantum computer executes a sequence of unitary transformations, $U_1 \dots U_n$, as specified by a quantum
 394 algorithm, with each transformation acting on one or two (rarely three) qubits. The unitary transformation
 395 is executed by a "gate", actually a physical operation that makes an external system (microwave or laser
 396 pulse, magnetic field switch, AC/DC signal) to interact with the qubit to modify its state. For a single
 397 qubit it is often a rather simple operation, for example a microwave pulse at the exact frequency of the J-J
 398 junction. For two-qubit gates it may be more complicated, since qubits are in principle arranged in such a
 399 way that do not interact with each other, in their ground state. Coupling can be realized for example by
 400 properly designing the capacitance between the pair (Yamamoto et al. (2003)), or through their mutual
 401 inductance (Hime et al. (2006)), or by a microwave cavity in which confined photons transfer the quantum
 402 state between qubits (Majer et al. (2007)), or yet by other means.

403 One-qubit gates act on either the phase or the excitation energy of a single qubit by applying a rotation
 404 on the Bloch surface (Fig.2b). The states of the qubit can be represented as column vectors, $|0\rangle = \begin{pmatrix} 1 \\ 0 \end{pmatrix}$
 405 and $|1\rangle = \begin{pmatrix} 0 \\ 1 \end{pmatrix}$. Then the simplest operations of transformation of the state (a "gate") can be schematized
 406 by 2×2 matrices. An arbitrary rotation of the qubit state about an axis $\hat{\mathbf{n}}$ is represented as $U_{\hat{\mathbf{n}}}(\phi) =$

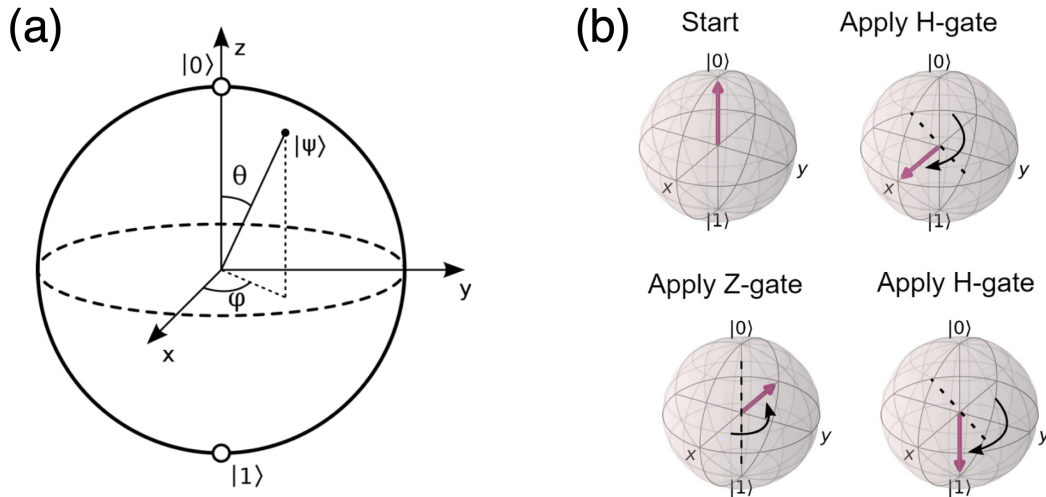


Figure 2. (a) The Bloch sphere. (b) Schematic of the transformation on the Bloch surface corresponding to the sequential application of a H , Z and again a H gate, resulting in the spin flip from $|0\rangle$ to $|1\rangle$ (therefore equivalent to an X gate).

407 $\exp(-i\phi\hat{n} \cdot \vec{\sigma}) = \cos(\phi)\mathbf{I} - i \sin(\phi)(\hat{n} \cdot \vec{\sigma})$, with $\vec{\sigma}$ the block vector having the Pauli matrices as its xyz
 408 components.

409 In the case of the TransMon, standard rotation gates are available (hardware implemented) in the xy -plane
 410 or in the z -axis. For the xy single-qubit gate, the Hamiltonian reads:

$$\mathcal{H} = -\frac{\hbar}{2}\omega_{01}\sigma_z + W \cos(\omega_R t - \phi)\sigma_x = -\frac{\hbar}{2} [\Delta\sigma_z - W(\cos \phi\sigma_x + i \sin \phi\sigma_y)] \quad (6)$$

411 When the MW frequency is exactly tuned to the qubit frequency it is $\Delta=0$, and the rotation in the xy
 412 plane is fixed only by the choice of the phase angle ϕ . This makes the xy or phase-gate one of the most
 413 important elements of quantum computing.

414 Students may find it difficult to grasp the meaning of the phase gate, since in introductory classes of
 415 quantum mechanics the role of the phase remains rather obscure, and is often swept under the carpet by
 416 noticing that "phase disappears when taking the $|\psi|^2$ of the wavefunction".³ If the output of a measurement
 417 is a random distribution, in a classical setting one can only accumulate probability amplitudes of each
 418 instance; however, in the quantum calculation, constructive or destructive interference allows to amplify or
 419 suppress some of the outputs, by manipulating the phases of the qubits. A great example is the quantum
 420 Fourier transform (QFT) which finds periodic instances in a sequence, just like its classical counterpart.
 421 The QFT algorithm transforms a m -bit state $|\psi\rangle = \sum_i \alpha_i |i\rangle$ to $|\psi'\rangle = \sum_i \beta_i |i\rangle = \sum_i \sum_k \alpha_i e^{2\pi i \phi_k} |i\rangle$,
 422 $i, k = 1 \dots m$. It requires the application of one Hadamard gate to each pair of qubits, followed by a sequence
 423 of phase-gates for each term in the k -sum, resulting in a total of m Hadamard + $m(m + 1)/2$ phase-gates
 424 (that is, $\mathcal{O}(m^2)$ polynomial complexity).

³ This may be true for pure states and for many expectation values, such as energy, but it is not always the case. Consider, e.g., the mixed state $\psi = a_1\phi_1 + a_2\phi_2$: its $|\psi|^2 = |a_1|^2|\phi_1|^2 + |a_2|^2|\phi_2|^2 + (a_1^*a_2\phi_1^*\phi_2 + c.c.)$ depends on the phase, since $a_1^*a_2 = |a_1||a_2|e^{i(\theta_2 - \theta_1)}$. The energy of such a mixed state has periodic oscillations at the frequency $\omega = (E_2 - E_1)/\hbar$ because of the rotating phase.

425 Two-qubit gates carry out controlled transformations of the second qubit state (*target*), conditioned by
 426 the state of the first one (*control*). Compared to single-qubit gates, whose working speed is limited by the
 427 strength of the driving fields (Frey (2016)), two-qubit gates (notably, the entangling gate) can only operate
 428 at a speed proportional to the interaction strength between the qubits (Schäfer et al. (2018); Steane et al.
 429 (2014)). This is typically weaker than available single-qubit drive strengths and cannot be easily increased,
 430 thereby representing one important limit to the coherence time (see below). For the SC qubits, moreover,
 431 the limited anharmonicity makes single-qubit gates not much faster than two-qubit gates (Stehlik et al.
 432 (2021); Moskalenko et al. (2022)).

433 As the two-qubit state is a column vector of dimension 4, the gates can be written as a 4x4 matrix. The
 434 controlled transformations can be of two main types: the Controlled-NOT (CNOT), which leaves $|00\rangle$
 435 and $|01\rangle$ unaltered, and swaps $|10\rangle$ and $|11\rangle$; the Controlled-Phase (CPHASE), which flips the phase of
 436 the two-qubit state if both the qubits are excited. It is interesting to note that CNOT can be constructed
 437 by applying Hadamard to the target qubit, then CPHASE to this new state, and Hadamard again (see e.g.
 438 Wallquist et al. (2005)). The ensemble of CNOT gate, the Hadamard, and all phase gates, form an infinite
 439 set of *universal* gates, by which any m -qubit unitary operation can be represented using $\mathcal{O}(m4^m)$ such
 440 gates.

441 **Entanglement.** It is worth noting once more that *coupling* is not the same thing as *entanglement*. The
 442 coupling refers to the physical mechanism allowing the exchange of information between different qubits.
 443 The result can be either a non-entangled, a partially-, or a maximally-entangled state vector $|\psi\rangle$ (Franco and
 444 Compagno (2016)). **If $\rho^2=\rho$, with $\rho=|\psi\rangle\langle\psi|$, the state is pure by definition. To check if it is also entangled,**
 445 **however, we may look at the purity of the respective substates describing its parts. Imagine a system divided**
 446 **in two parts with coordinates q_1, q_2 , and in a pure state $|\psi_{12}\rangle = |\psi(q_1, q_2)\rangle$ such that $\rho_{12} = |\psi_{12}\rangle\langle\psi_{12}|$;**
 447 **each subsystem lives in a state described by the reduced density $\rho_1 = \text{Tr}_2\{\rho_{12}\}, \rho_2 = \text{Tr}_1\{\rho_{12}\}$. Then,**
 448 **if the state wavefunction is not factorizable into pure states for 1 and 2, $|\psi_{12}\rangle \neq |\psi_1\rangle \otimes |\psi_2\rangle$, the two**
 449 **subsystems are entangled, and their respective reduced density describes a mixed state for each part (Caban**
 450 **et al. (2015)). When a state is written out as a sum of basis vectors it is not always obvious to decide whether**
 451 **or not it is separable. For example, a general two-qubit pure state like $|\psi\rangle = a|00\rangle + b|01\rangle + c|10\rangle + d|11\rangle$,**
 452 **is separable when $a=b=c=d$, as $|\psi\rangle = a(|0\rangle + |1\rangle)(|0\rangle + |1\rangle)$, and not separable (entangled) for, e.g., $b=c=0$,**
 453 **since both qubits are now in a mixture of $|0\rangle$ and $|1\rangle$.**

454 The differences here are subtle, and worth explaining. *Separable* states can be written as a combination
 455 of *product* states; product states, in turn, can be written as direct product \otimes of quantum states living in each
 456 subspace. Product states have no correlation at all among the degrees of freedom of the subspaces, whereas
 457 separable states can have correlations, which however are entirely classical. *Entangled* states have a higher
 458 degree of correlation of purely quantum origin.

459 Maximally-entangled states are called "Bell states". The meaning of maximum entanglement is usually
 460 taken as the maximization of Von Neumann's entropy (see below, Eq.(27) and on). A more layman
 461 interpretation is that the state is described by a single wavefunction (i.e., not separable), so that a
 462 measurement of any qubit gives the values of all the others deterministically. (By contrast, a mixed
 463 state would give a statistical mixture of all qubits.)

464 Entangled states can be obtained by the sequential application of a Hadamard single-qubit gate, followed
 465 by a CNOT. The Hadamard produces a 50/50 superposition of the basis states, for example:

$$[H]|0\rangle = \frac{1}{\sqrt{2}} \begin{pmatrix} 1 & 1 \\ 1 & -1 \end{pmatrix} \begin{pmatrix} 1 \\ 0 \end{pmatrix} = \frac{1}{\sqrt{2}} \begin{pmatrix} 1 \\ 1 \end{pmatrix} = \frac{|0\rangle + |1\rangle}{\sqrt{2}} \quad (7)$$

466 Then, the CNOT gate operates on the product states, such as $|\psi_p^\pm\rangle = \frac{1}{\sqrt{2}}(|0\rangle \pm |1\rangle) \otimes |p\rangle$, $p = 0, 1$ to
 467 obtain the finally entangled states. For example:

$$[CNOT]|\psi_0^+\rangle = \frac{1}{\sqrt{2}} \begin{pmatrix} 1 & 0 & 0 & 0 \\ 0 & 1 & 0 & 0 \\ 0 & 0 & 0 & 1 \\ 0 & 0 & 1 & 0 \end{pmatrix} \begin{pmatrix} 1 \\ 0 \\ 1 \\ 0 \end{pmatrix} = \frac{1}{\sqrt{2}} \begin{pmatrix} 1 \\ 0 \\ 0 \\ 1 \end{pmatrix} = \frac{1}{\sqrt{2}} (|00\rangle + |11\rangle) \quad (8)$$

468 For two qubits, the four possible Bell states obtained by combining all product states are given by:

$$|\psi_B^\pm\rangle = \frac{1}{\sqrt{2}} (|00\rangle \pm |11\rangle) \quad (9)$$

$$|\phi_B^\pm\rangle = \frac{1}{\sqrt{2}} (|01\rangle \pm |10\rangle)$$

469 However, not all entangled states are Bell states. For example, the states $|\psi\rangle = \cos(\theta)|00\rangle + \sin(\theta)|11\rangle$
 470 for $\theta \in (0, \pi/4)$ are all entangled but are not Bell-states.

471 A last point worth noting, is that the time profile of the interaction Hamiltonian is controlled by classical
 472 parameters, such as the intensity of a laser beam, the value of the gate voltage, or the current intensity in a
 473 wire. Of course, all such parameters are also quantum-mechanical in nature, when examined at the atomic
 474 level; the fact that they behave classically means that there should be no entanglement between their (very
 475 large) quantum states, and the internal states of the qubits of the quantum computer.

476 **Decoherence, dephasing, thermalization.** However, all physical quantum systems are subject to
 477 decoherence and dissipation, mainly arising from their noisy interaction with the environment. As we
 478 will see later (Section 5), when exploring the connection between thermodynamics and information, any
 479 realistic sequence of operations of a quantum information processing device is irreversibly accompanied
 480 by the production of entropy, which pairs with the irretrievable loss of (quantum) information into the
 481 environment. Then, some questions immediately appear:

- 482 • What are the physical limitations on information processing set by thermodynamics?
 483 • Can we maintain quantum computers in the deep quantum regime, so that we can actually exploit their
 484 advantage w/r to classical computers?
 485 • The exponential increase in computing capability will entail and exponential increase of thermodynamic
 486 work and dissipated heat?

487 Within a standard picture for spin-1/2 systems, there are two characteristic decay rates that contribute to
 488 coherence loss: $\Gamma_1 = 1/T_1$ is the longitudinal relaxation rate (an energy decay rate), that is the time over
 489 which the qubit exchanges energy with its environment; $\Gamma_2 = 1/T_2 = 1/(2T_1 + 1/T_\phi)$ is the transverse

490 relaxation rate (a decoherence rate), that is the time over which the device remains phase-coherent. In
 491 simpler words, T_1 is the time taken by a qubits to decay spontaneously e.g. from $|1\rangle$ to $|0\rangle$, while T_2 is
 492 where a qubit dephases into a mixture of states such that the phase can no longer be accurately predicted.
 493 Over the past 20 years, a steady increase in T_2 has brought superconducting qubits from the stage of
 494 laboratory experiments, to the capability of building the first quantum computers (Oliver and Welander
 495 (2013); Gil and Green (2020)).

496 Currently the error rate on the best quantum computers is about 1% for each elementary operation.
 497 Although a 99% accuracy may seem already high, a single mistake affects the whole entangled system: just
 498 one error corrupts the result. One way to improve errors could be to replicate N identical copies of the
 499 logical unit and have them "vote" on the output. Only if all N physical qubits give the same answer, the
 500 logical qubit is correct. (This is similar to what happens in classical computers, e.g. with the Hamming
 501 correction code.)

502 Another method that is becoming standard is the introduction of correction, or "ancilla", qubits, with the
 503 same logic of the parity bit in classical digital computers. The ancilla qubit is prepared in $|0\rangle$, and then a
 504 sequence of CNOT gates are applied, from the working qubits onto the ancilla qubit. These gates flip the
 505 ancilla or "check bit" between $|0\rangle$ and $|1\rangle$ an even or odd number of times, depending on the parity of the
 506 bit string stored in the data qubits. When the ancilla qubit is measured, the parity of the state is the only
 507 thing that is measured, without interfering with the rest of the quantum computation.

508 However, as the number of logical qubits grows, the number of layers to correct the original plus the
 509 correction qubits grows exponentially. Google's labs estimate is that current technology may require 1,000
 510 physical qubits to encode 1 logical qubit and attain an error rate of 1 in 10^9 .

511 Introduced as a measure of the practical estimate of the minimal availability of quantum resources to
 512 perform a computation, the *quantum volume* of a quantum computer depends on the number of qubits N , as
 513 well as the number of steps that can be executed while remaining in a coherent state, that is the *circuit*
 514 *depth*, d :

$$V_Q = \min[N, d(N)]^2 \quad (10)$$

515 The variation of d with the number of qubits is $d(N) \simeq 1/(N\epsilon)$, for an average error rate ϵ . However, a

516 quantum algorithm typically engages subsets of n qubits from those available in the whole machine N .
 517 IBM's modified definition of quantum volume (Moll et al. (2018)) is the equivalent complexity to simulate
 518 the same quantum circuit on a classical computer:

$$\log_2 V_Q = \max_{n \leq N} \{ \min[n, d(n)]^2 \} \quad (11)$$

519 Such definitions only provide a measure of the theoretical feasibility of a computation, neglecting other

520 constraint factors as, e.g., read-out times, $1/f$ noise, quantum error correction, magnetic or current (phase)
 521 fluctuations.

4 THERMODYNAMICS IN A CLASSICAL DIGITAL COMPUTER

522 Thermodynamics was developed in the XIXth century, to provide a unified framework between mechanical
523 sciences and **calorimetry**. **At the time, the motivation was very practical, namely use differences of**
524 **temperature to generate heat that could** put bodies into motion - as clearly indicated by its name, *thermo*
525 (heat) and *dynamo* (movement). In other words, the goal was to design and optimize thermal engines, i.e.
526 devices that exploit the transformations of some “working substance” between different temperatures, to
527 convert heat into work. Work and heat are two ways to exchange energy, according to the First Law of
528 thermodynamics it is possible to convert one into another.

529 However, turning heat into work and back into heat, comes at a cost: it is not possible to cyclically extract
530 work from a single hot bath (Kelvin 1851), **and while any amount of work can generate the same amount**
531 **of heat, heat can never be converted into the same amount of work.**⁴ This no-go statement is one of the
532 expressions of the Second Law of thermodynamics, which ultimately deals with irreversibility. Interestingly,
533 the concept of work came originally from mechanical sciences (Lazare Carnot, 1803) and represents a
534 form of energy that can be exchanged reversibly: in principle, there is no time arrow associated with
535 work exchanges (at least for conservative forces), since the equations of motion in classical mechanics are
536 perfectly time-reversible. But when building steam machines it is always found that heat Q spontaneously
537 flows (only) from hot to cold bodies. To extract work W , a source and a sink at different temperatures T_1
538 and T_2 are necessary, independently on the nature of the exchange medium, as stated by Sadi Carnot in
539 1823 in a idealized experiment, the “Carnot cycle”, for which he derived a theorem regarding the efficiency
540 of a machine producing work.

541 A Carnot cycle is a closed ensemble of operations by which a thermodynamic machine starts from a
542 condition and returns to the same condition, after having performed some work at the expenses of the heat
543 extracted from a source at higher temperature than a sink. The theorem states that the ideally reversible
544 engine produces work from heat if and only if the sink temperature is lower than the source’s, $T_2 < T_1$.
545 If $T_2 > T_1$ work must be supplied to the engine. If on the other hand $T_1 = T_2$ no work can be extracted.
546 Being in theory fully reversible and designed to have the maximum possible thermodynamic efficiency, the
547 Carnot cycle can be run in the “forward” direction and “in reverse”. When running in the opposite direction,
548 the same amount of work performed in the forward cycle is returned to the source as heat, **the sum of the**
549 **forward and reverse operation resulting in zero net energy consumed and zero net work extracted. All such**
550 **considerations, however, remain in the domain of idealized systems.** The practical problem with such an
551 ideal situation is that the heat is extracted from the source, and transferred to the sink, while remaining at
552 constant temperature, T_1 and T_2 , apparently contradicting the experimental observation that Q only flows
553 from hot to cold bodies. Furthermore, to move from T_1 to T_2 and back, a rigorously **lossless transformation**
554 **is required**, which in practical terms means to proceed at infinitely slow rate.

555 **Entropy is the name we give to our losses (Clausius, 1856).** The Second Law of thermodynamics is quite
556 different from other laws in physics, since (i) there are many different statements for the same law, and
557 (ii) it is only a qualitative description, rather than a quantitative relationship between physical quantities.
558 Clausius wanted to put Carnot’s theorem on a more general basis, considering that heat exchanges between
559 a body and a thermal bath are always *not* reversible in the real world, and imply a loss of energy to the
560 environment. He introduced the notion of entropy, S , as the ratio between heat exchanged and working
561 temperature, encompassing both reversible and irreversible transformations in the single inequality:

⁴ Until around 1850 heat and work were considered to be distinct subjects. The experimentally observed asymmetry was the reason why Lord Kelvin initially did not accept the equivalence of work and heat, and rather expanded on Clapeyron’s theory of reversible heat engine (Saslow (2020)).

$$Q \left(\frac{1}{T_{low}} - \frac{1}{T_{high}} \right) = \Delta S \geq 0 \quad (12)$$

562 Hence, it is usually said that the Second Law of thermodynamics introduces the notion of a time arrow.

563 Here we already could start thinking of the analogy with the operations being carried out in a digital
 564 computer, accompanied by a waste of heat. The computer is in principle maintained at constant temperature,
 565 however it is an engine consuming energy to perform a computation, and its temperature would increase
 566 (in the absence of refrigeration and heat removal) at each operation performed. This energy goes into flow
 567 of electrons that move around the integrated circuits, capacitors, resistances, connecting wires. We can use
 568 Maxwell equations to deduce the amount of power accompanying the current. However, the fundamental
 569 operations that the computer is doing are creating and destroying information, by using this electrical
 570 current to flip the bit states in its memory from 0 to 1 and vice versa. Is there a link between the logical
 571 operations of creating and destroying information, and the energy required to physically run the computing
 572 machine?

573 **Statistical mechanics definition of entropy (Boltzmann 1875).** In order to make such a link, we must at
 574 least be able to find a connection between the macroscopic world of thermodynamics, and the microscopic
 575 world in which electrons move and collide with other electrons and lattice vibrations (phonons). The
 576 connection between the macroscopic and microscopic degrees of freedom was attempted by Boltzmann, by
 577 introducing the notion of *micro-state*, that is a definition of the instantaneous condition of the microscopic
 578 degrees of freedom (i.e., positions and momenta) that make up a macroscopically observable state. As
 579 it is immediately evident, a macroscopic state can be obtained in a variety of microscopic ways: the air
 580 molecules in a room continuously change their micro-state while the overall temperature and pressure
 581 remain constant.

582 Boltzmann introduced the following microscopic expression for the entropy, interpreted as an extensive
 583 function that "counts" the number of micro-states of the system:

$$S = k_B \ln \Omega \quad (13)$$

584 Ω is the number of microscopic states compatible with a given set of thermodynamic constraints

585 (T, P, V, N, \dots) . Ω is a very difficult quantity to compute, or even to estimate, except some very simple
 586 cases, such as the perfect gas:

$$\Omega = \frac{1}{N!} (2mE)^{3N/2} V^N \quad (14)$$

587 This statement is valid in the "microcanonical" statistical mechanics ensemble at constant- $\{N, V, E\}$.

588 For this experimental set up, all micro-states are equiprobable at equilibrium.

589 By contrast, for constant- $\{N, V, T\}$ conditions, that is the "canonical" ensemble, micro-states are not
 590 equiprobable, but are distributed according to the Boltzmann probability $\exp(-E/k_B T)$, and the energy E
 591 is replaced by $k_B T$ in the definition of Ω , since T is now constant and all energy values E are allowed. That
 592 is, energy can fluctuate. Fluctuating quantities are not usually considered in macroscopic thermodynamics,

593 which deals with average values at equilibrium. Macroscopically we expect a system to have both a
 594 well-defined temperature and well-defined energy. When we look at the microscopic scale, for a given
 595 temperature the energy can fluctuate between different values. The macroscopic condition is recovered
 596 because energy fluctuations ΔE are proportional to the (square root of) specific heat, an intensive quantity
 597 proportional to the number of degrees of freedom N of the system:

$$(\Delta E)^2 = k_B T^2 N c_V \quad (15)$$

598 Hence, when we calculate the relative importance of energy fluctuations with respect to the absolute
 599 value of the intensive quantity energy, it is $\Delta E/E \propto \sqrt{N}/N = 1/\sqrt{N}$. In other words, in the limit of a
 600 macroscopic system $N \sim 10^{24}$ the energy is practically constant. Eq.(15) is an example of a fluctuation-
 601 dissipation relation, establishing a relationship between the thermal fluctuations of a physical quantity
 602 (energy) and another quantity (the specific heat) that describes its dissipation.

603 **CMOS power dissipation: how big is a bit?** Logical units in digital computers are made by combining a
 604 number of transistors, carved with high density in the silicon chip. When the transistor is in a given logical
 605 state its current consumption is negligible. All energy dissipation takes place during transitions between
 606 logical states, and the source of this dissipation is the need to charge or discharge the related capacitors.
 607 The energy dissipated to charge/discharge one CMOS transistor has a well established form:

$$E_{switch} \simeq \alpha C_{node} V^2 \simeq 0.01 \cdot 10^{-12} \cdot (3)^2 \simeq 0.1 \text{ pJ} \simeq \mathcal{O}(10^7) k_B T \quad (16)$$

608 for a supply voltage of 3 V, C_{node} being the lumped capacitance, and α a coefficient including the clock
 609 frequency (Wiltgen et al. (2013)). In the Xeon Broadwell-E5 (14-nm technology) about 7,2 million
 610 transistors arranged in about 1 million logic gates (making up CPU, memories, controllers, etc.), are packed
 611 in 456 mm². Therefore, each transistor covers about $8 \times 8 \mu\text{m}^2$, with a thickness of ~ 0.2 nm, that is about
 612 150 billion Si atoms. So, each atom dissipates about $10^{-4} k_B T$ at each switching of the transistor.

613 However, switching is a collective, statistically uncorrelated process: atoms follow quantum mechanics,
 614 currents follows Maxwell's equations. A question arises: is there a link between the heat dissipation and
 615 the use/transfer/loss of information?

616 **Thermal noise and random bit flips.** The flow of electrons in any current-conducting medium, for example
 617 across a resistor, is affected by thermal fluctuations that entail a voltage fluctuation, with a spectrum usually
 618 assumed to be Gaussian with zero mean. The Johnson-Nyquist formula (originally derived on the basis
 619 of the equipartition law, (Johnson (1928); Nyquist (1928))) gives the thermal noise power density as the
 620 product of thermal energy by the bandwidth, $P = k_B T \Delta f$. To fix a number, a 1 kOhm resistor at room
 621 temperature with a bandwidth of 1 Hz generates a RMS noise of 4 nV. Although a capacitor is ideally a
 622 noiseless device, when combined with resistors it generates noise. Due to the fact that Δf is inversely
 623 proportional to \sqrt{RC} , and given the steady reduction of the oxide layer with increasing transistor density,
 624 the overall result of CMOS miniaturization is an increase in the RMS width of the Gaussian voltage noise.

625 Under such conditions, there is a finite probability that a spike in the voltage noise V_n could pass, every
 626 now and then, the threshold voltage V_{th} to flip the bit, in a random fluctuation. The average frequency by

627 which such an event can occur can be estimated from the Rice formula (Rice (1945)), whose result in the
628 approximation of white-noise is:

$$\nu = \nu_0 \exp\left(-\frac{V_{th}^2}{2V_n^2}\right) \quad (17)$$

629 Due to the steep dependence on the square of the V_{th}/V_n ratio, the frequency of a random bit-flip is
630 estimated about 35 million per hour at $V_{th}/V_n \simeq 5$, and drops to 2 in 10^{-9} per hour (that is, about 20 errors
631 per hour in a 1-Gbyte RAM chip) at $V_{th}/V_n \simeq 10$ (Kish (2002)). In recent years the threshold voltage V_{th}
632 has been constantly reduced, proportionally to the decrease in supply voltage, and in the most advanced
633 CMOS circuits it could be of the order of ~ 0.45 V. Requiring the signal/noise voltage ratio to be at least
634 > 10 , implies that the RMS thermal voltage fluctuation must be kept below about 35 mV to ensure a safe
635 operation, or a maximum temperature of $T = eV_n/k_B \lesssim 150^\circ\text{C}$. Since leakage currents start affecting
636 silicon electronics above $\sim 180^\circ\text{C}$, random bit flipping is likely the main thermal limit to further decrease
637 of voltage, the peak temperature of hot-spots in dense multiprocessor arrays being in the $\sim 100\text{-}120^\circ\text{C}$
638 (normal electronics is rated to function up to 85°C , military electronics up to 125°C , which actually seems
639 a bit of a stretch, in view of the rapidly increasing bit-error rate).

5 INFORMATION AND THERMODYNAMICS: THE DEMONS OF LEO SZILARD

640 **“Information is physical” (R. Landauer, 1961).** One important achievement in the study of information
641 processing has been to make the link with thermodynamics, with the understanding that manipulating
642 information is inevitably accompanied by a certain minimum amount of heat generation. Computing, like
643 all processes proceeding at a finite rate, must involve some dissipation. More fundamentally, there is a
644 minimum heat generation per operation, independently on the actual rate of the process. The binary logic
645 devices of digital computers must have at least one degree of freedom associated with the information they
646 carry, typically a logic port with more than one input and just one output mixes information from the input
647 data, to present a value to the single degree of freedom of its output. As we will see below, devices with
648 more input ports than output ports are inherently irreversible, in that the output does not allow to reconstruct
649 the input information, Such devices exhibiting logical irreversibility are essential to classical computing.
650 The important point is that *logical* irreversibility implies *physical* irreversibility, which is accompanied
651 by dissipative effects. The Boltzmann expression, such as Eq.(14), makes a link between entropy and the
652 number of microstates available for a system at a given energy, showing that the larger is Ω , the larger the
653 distribution of possible configurations (in quantum terms, we could think of some analogy with mixed
654 states). The dynamical equations, perfectly reversible at the level of individual degrees of freedom, become
655 practically irreversible when the number of degrees of freedom gets very large. If we film two colliding
656 balls and play the movie in reverse, it is impossible to tell the past from the future. If however we film a
657 single ball hitting a triangle at snooker and play the same trick, it is immediately evident that the future is
658 the one with more disorder at the end: the larger Ω brings more entropy, and less information about the
659 dynamics of the individual trajectories. For a snooker with an Avogadro’s number of balls, the information
660 about past physical trajectories is irreversibly lost.

661 Rather than counting micro-states *à la* Boltzmann, entropy can also be rewritten (Gibbs, Jaynes (1965)) in
662 terms of the absolute probability of each micro-state:

$$S = -k_B \sum_i p_i \ln p_i \quad (18)$$

663 For the microcanonical ensemble in which all the $p_i = 1/\Omega$, this writing is exactly the same as

664 Boltzmann's Eq.(13) (which was actually put down in that form by Max Planck); for a distribution
665 $p_i = \exp(-E_i/k_B T)$, instead, it easily shown that the canonical ensemble is obtained with constant N , V
666 and T . Goldstein et al. (2020)

667 The notion of *information entropy* was defined by Shannon, Shannon (1948) when he tried to quantify the
668 "loss of information":

$$H = - \sum_i p_i \ln p_i \quad (19)$$

669 It can be viewed as the entropy change due to the presence/absence of information about a system, and

670 it actually was Von Neumann to suggest Shannon the evident equivalence between his definition and
671 Boltzmann's statistical mechanics formulation. But pushing the analogy even more forward, couldn't it
672 also be a measure of a *heat loss* accompanying the exchange of information?

673 **The Szilard engine.** Instead of considering a gas made of a large number of particles (Carnot), consider
674 just one single particle that is either on the left or on the right of a chamber equipped with two frictionless
675 "pistons" and a "wall". "Left" or "right" positions can be used to encode one bit of information (Figure
676 3). A "demon" who knows in which side of the box the particle is at time $t=0$, can spend this information
677 (entropy) to:

- 678 1. close the wall between the two halves of the box; then
- 679 2. let the piston in the empty side move by doing zero work, until reaching the closing wall; and finally
- 680 3. extract useful work, by opening the wall and leaving the particle to expand back (isothermally) to its
681 original equilibrium volume.

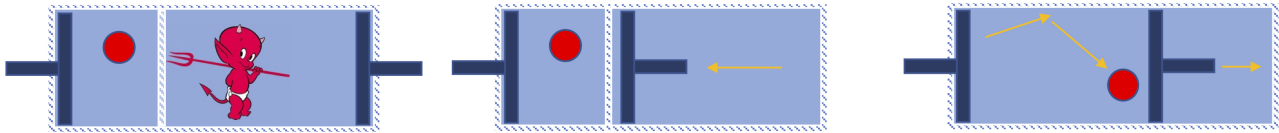


Figure 3. The Szilard engine and its demon.

682 This thought experiment was designed in 1929 by Leo Szilard (Szilard (1929)), to prove that possessing
 683 and using pure information has measurable thermodynamic consequences. Denoting by p the probability
 684 that the particle is (for example) found on the left, the Shannon entropy for the 1-particle engine reads:

$$H[p] = -p \ln p - (1 - p) \ln(1 - p) \quad (20)$$

685 If the demon has zero information, then: $p = (1 - p) = 1/2$, and $H[p] = -\ln 1/2 = \ln 2$. But if the
 686 demon has this 1 bit of information, H must go to zero upon completing the cycle and:

$$\Delta H = H_{fin} - H_{in} = -\ln 2 \quad (21)$$

687 Using the single bit of information thus corresponds to a *reduction* in the entropy of the system. The
 688 global system entropy is not decreased, but information-to-free-energy conversion is possible. After the
 689 particle is confined in one side of the box, the system is no longer in equilibrium: it appears that using
 690 information changed the system state without apparently changing the energy. Notably, the Szilard engine
 691 has been recently realized experimentally, by using Brownian particles (Toyabe et al. (2010)) or single
 692 electrons (Koski et al. (2014)).

693 (To be fair, the demon should have indeed more than just one bit of information: he must firstly decide at
 694 what place to put the wall, and then control the piston's direction of motion. Therefore, at least 3 bits of
 695 information are required.)

696 Let us then consider a "computer" with N binary bits. In the initial (prepared) all-zero state, all the $p_i = 1$
 697 and :

$$H_{in} = -N \ln 1 = 0 \quad (22)$$

698 After thermal equilibration, each bit has equal probability $p_i = 1/2$ of being found in the state 0 or 1.
 699 This is to say that the initial information can be dispersed in any of the N states, and the information
 700 entropy is:

$$H_{fin} = N \ln 2 \quad (23)$$

701 When we restore the initial state (that is, flush all voltages to ground, and reset all bits to 0) a minimum
 702 heat of:

$$\Delta Q = k_B T \Delta H = k_B T N \ln 2 \quad (24)$$

703 is wasted. The RESET operation (erasure) is irreversible, and the wasted information turns to heat. The
 704 huge difference between the theoretical $\ln 2$ and the $\mathcal{O}(10^9)k_B T$ observed for the heat dissipation of a real
 705 transistor is due to the accessory circuits and wiring around each bit of information, but the lower limit of
 706 $\ln 2$ is incompressible.

707 To check this absolute limit, imagine that our computer goes instead into a defined final configuration,
 708 in which some bits have a higher probability of being in a given state, as could be in the result of some
 709 calculation. For example, $N/2$ have $p = 3/4$ and $N/2$ have $p = 1/4$ of being in state 1 (and all have $1 - p$
 710 probability of being in 0):

$$H_{fin} = \Delta H = -\frac{N}{2} \ln \frac{3}{4} - \frac{N}{2} \ln \frac{1}{4} = N \left(\ln 4 - \ln 3^{1/2} \right) > N \ln 2 \quad (25)$$

711 It is easily shown that any choice of p_i 's different from $1/N$ gives a larger entropy. The value of $\ln 2$
 712 appears therefore as an absolute lower bound for the heat dissipated by an operation destroying the
 713 information of a single bit.

714 For quantum systems, the statistical state is described by the density matrix ρ . The probability to have a
 715 certain state $|n\rangle$ out of a complete basis, as the outcome of a measurement, is $p_n = \langle n | \rho | n \rangle$. Therefore,
 716 the (Shannon) information entropy for such a measurement is:

$$S(\rho) = \sum_n \langle n | \rho | n \rangle \ln (\langle n | \rho | n \rangle) \quad (26)$$

717 By changing to the basis in which the density matrix is diagonal, the entropy assumes its minimum value,
 718 and is called the Von Neumann entropy:

$$S_{VN}(\rho) = -\text{Tr}\{\rho \ln \rho\} \quad (27)$$

719 usually multiplied by the constant k_B to give the entropy energy-like units. Evidently, the Von Neumann
 720 entropy can be identified with the information entropy only if we pretend to know beforehand in which basis
 721 ρ is diagonal. For an equilibrium state with Hamiltonian \mathcal{H} , this is the canonical state, $\rho = \exp(-\beta\mathcal{H})$. A
 722 rigorous definition of entropy, however, should not assume any special *a priori* basis. At least the (classical)
 723 uncertainty of the macroscopic measurement apparatus should be included, the quantum state entropy
 724 being written as a conditional probability $S(\rho|\mathcal{A})$ of obtaining a certain measurement outcome for a given
 725 measurement condition, and averaged over all the measurable results \mathcal{A} (Stotland et al. (2004)):

$$\langle S(\rho|\mathcal{A}) \rangle_{\mathcal{A}} = S(\mathcal{A}) + \sum_{\mathcal{A}} P(\mathcal{A}) S(\rho|\mathcal{A}) \quad (28)$$

726 where $\langle \dots \rangle_{\mathcal{A}}$ indicates ensemble averaging, $P(\mathcal{A})$ is the probability of finding the macroscopic measurement

727 apparatus in the condition \mathcal{A} , and $S(\mathcal{A})$ the corresponding classical entropy.

728 **Landauer's Principle (classical).** Logical irreversibility is the act of processing an information in which
729 the output does not uniquely permit to retrieve the inputs. Now, the link between Gibbs' and Shannon's
730 definitions of entropy is a purely mathematical one: by dealing with two very different situations, different
731 variables and different processes, they arrive at two definitions of a measurable quantity that formally read
732 identical. A plausible deduction is that these should be therefore the same quantity. Landauer (Landauer
733 (1961)), and later Bennett (Bennett (1982)), tried to put the equivalence on more physical grounds. Their
734 idea was that information at its most basic stage is a distribution of 0's and 1's physically entrusted to a set
735 of bistable systems described by a bistable potential; then, the (classical) thermodynamics of each two-state
736 system automatically associates the processing of information with the thermodynamics laws that those
737 physical systems ought to follow. As a result, Shannon, Gibbs and Clausius' entropies *must* describe the
738 same thing, and logical irreversibility *must* imply thermodynamic irreversibility in the sense of the Second
739 Law, that is, increase of entropy (Ladyman et al. (2007)).

740 The only nontrivial reversible operation a classical computer can perform on a single bit is the NOT
741 operation, with one input and one output whose values are strictly defined. By contrast, the operations
742 AND, NAND, OR and XOR are all irreversible, since they have more than one input and just one output.
743 Hence, from the output of these logic gates we cannot reconstruct the input: information is irreversibly
744 lost. However, in a quantum computer irreversible operations may be - at least ideally - avoided, for
745 example by saving the entire history of the process, or by replacing the irreversible gates by more complex
746 but reversible gates, e.g. using a Toffoli gate instead of the AND. It seemed therefore that information
747 processing at the quantum level should have no intrinsic thermodynamic cost, as firstly Bennett (Bennett
748 (1982)) and then Feynman observed (Feynman (1985)).

749 But the operation of erasing a bit of information, instead, has two possible states (0 or 1) being mapped
750 to a single definite state of 0, so it must entail a loss of entropy since the value 0 has now $p=1$, for both
751 a classical or a quantum computer. A reformulation of the Second Law, Landauer's principle states that
752 the entropy decrease of the information-carrying degrees of freedom must always be compensated by an
753 equal (or greater) entropy increase in the environment. **Classical experiments in which the minimum heat
754 dissipated to erase the initial state, with a colloidal particle optically trapped in a double well representing
755 the two memory states, beautifully confirmed the link between information theory and thermodynamics
756 (Bèrut et al. (2011)).**

757 **Quantum computation is microscopically reversible.** Qubits are defined as two-state quantum systems,
758 described by a state vector in a 2-dimensional Hilbert space, spanning a closed surface with conserved
759 norm (i.e., the Bloch sphere). A standard basis is defined by two vectors $|0\rangle$ and $|1\rangle$, conventionally aligned
760 with the positive and negative direction of the z-axis.

761 In principle, a quantum gate performs rotations in the Bloch sphere of one or more qubits onto which it is
762 applied. Therefore, any quantum gate is a unitary operator:

$$UU^\dagger = U^\dagger U = \mathbf{I} \quad (29)$$

763 \mathbf{I} being the identity operator. Such operation conserves the norm of the quantum state, and is perfectly
764 time-reversible (Bennett (1982); Feynman (1985)). Upon application of any sequence of quantum gates,

765 state vectors span the whole surface of the Bloch sphere. Being unitary, qubit rotations (in principle) do not
766 generate any heat.

767 A *pure* quantum state is one that cannot be written as a probabilistic mixture of other quantum states.
768 Pure states can also result from the superposition of other pure quantum states (entanglement). A density
769 matrix, $\rho = |\psi\rangle\langle\psi|$, can be used to represent both pure ($\rho^2 = \rho$) and mixed ($\rho^2 \neq \rho$) states. Let's look for
770 example at two states in the 2-dim Hilbert space of a qubit, $|\psi_1\rangle = \begin{pmatrix} 1 \\ 0 \end{pmatrix}$ and $|\psi_2\rangle = \begin{pmatrix} 0 \\ 1 \end{pmatrix}$. Then, for a mixed
771 state with equal probabilities $p_i = \frac{1}{2}$ we have:

$$\rho = \sum_i p_i |\psi_i\rangle\langle\psi_i| = \frac{1}{2} \begin{pmatrix} 1 & 0 \\ 0 & 1 \end{pmatrix} \quad (30)$$

772 On the other hand, for a pure state with equal amplitudes, $|\psi\rangle = \frac{1}{\sqrt{2}}(|\psi_1\rangle + |\psi_2\rangle)$, the density matrix is:

$$\rho = |\psi\rangle\langle\psi| = \frac{1}{2} \begin{pmatrix} 1 & 1 \\ 1 & 1 \end{pmatrix} \quad (31)$$

773 In the Bloch sphere representation of a qubit, each point on the unit sphere stands for a pure state. The
774 arbitrary state for a qubit can be written as a linear combination of the Pauli matrices ($\hat{\sigma}_x, \hat{\sigma}_y, \hat{\sigma}_z$), with
775 three real numbers (r_x, r_y, r_z) as the coordinates of a point in the sphere:

$$\rho = \frac{1}{2} (\mathbf{I} + r_x \hat{\sigma}_x + r_y \hat{\sigma}_y + r_z \hat{\sigma}_z) \quad (32)$$

776 Points for which $r_x^2 + r_y^2 + r_z^2 = 1$ lie on the surface, and represent pure states of any superposition of
777 $|\psi_1\rangle = \begin{pmatrix} 1 \\ 0 \end{pmatrix}$ and $|\psi_2\rangle = \begin{pmatrix} 0 \\ 1 \end{pmatrix}$. Any other combination of $r_x^2 + r_y^2 + r_z^2 < 1$ lies in the interior of the sphere,
778 and represents thermally-mixed states.

779 How can we get thermally mixed states starting from pure states, and perform unitary transformations
780 that should not generate any heat loss?

781 **Pure states vs. mixed states: quantum entropy.** The time evolution of a pure state starting from ρ^0 at
782 time $t = 0$ under the action of a unitary operator $\hat{U}(t) = \exp(-i\mathcal{H}t/\hbar)$ is obtained from the Von Neumann
783 equation:

$$\frac{d\rho}{dt} = -\frac{i}{\hbar} [\mathcal{H}, \rho] \quad (33)$$

784 (that is, the quantum-equivalent of Liouville's equation) as :

$$\rho^t = U(t)\rho^0 U^\dagger(t) \quad (34)$$

785 For a time-independent Hamiltonian it is easily shown that the density matrix elements evolve as:

$$\rho_{nm}(t) = e^{-i\omega_{nm}(t-t_0)} \rho_{nm}(t_0) \quad (35)$$

786 The intrinsic dynamics generated by this time evolution is unitary, i.e. the diagonal density ρ_{nn} is
 787 conserved in time, and the coherent superpositions oscillate at the frequencies ω_{nm} . The Von Neumann
 788 entropy, Eq.(27), is as well invariant under unitary dynamics (in fact, for pure states this $S(\rho)$ is just zero).
 789 This means that entropy generation by irreversibility cannot be a result of the intrinsic quantum dynamics.
 790 It can only result from changes in time of the statistical description of the interaction with an external
 791 system, which turns pure states into mixed states.

792 The density matrix of a mixed state can be defined on the basis of all the pure states $|\psi_i\rangle$ as :

$$\rho = \sum_i p_i |\psi_i\rangle \langle \psi_i| \quad (36)$$

793 and the Von Neumann quantum entropy of the mixed state, by extension, is obtained as :

$$S_{VN}(\rho) = -k_B \text{Tr} \{ \rho \ln \rho \} = -k_B \sum_i p_i \ln p_i \quad (37)$$

794 For two entangled subsystems A and B (for example two qubits, or an atom and an external field) a
 795 quantity of interest is the Araki-Lieb inequality (Araki and Lieb (1970)):

$$|S_A - S_B| \leq S_{AB} \leq S_A + S_B \quad (38)$$

796 For a pure state, the partial trace tells that the entropy is equal for the two subsystems $S(\psi) =$
 797 $-\text{Tr} \rho_A \ln \rho_A = -\text{Tr} \rho_B \ln \rho_B$. The inequality (38) gives the same result, because the total wavefunction
 798 is also a pure state, therefore $S_{AB} = 0$, which implies $S_A = S_B$. This may be very useful e.g. for the case
 799 of an spin-1/2 atom interacting with an external field: while the entropy of a two-state system is easy to
 800 calculate, the entropy of the field could be much more difficult to obtain. It has been recently demonstrated
 801 that the same Araki-Lieb inequality can be extended to mixed states (Anaya-Contreras et al. (2019)).

6 QUANTUM THERMODYNAMICS IS NOT WHAT YOU THINK

802 It is both interesting and funny to think that, to some extent, quantum mechanics was born out of
 803 thermodynamic considerations. The energy quantum was introduced in 1900 by Max Planck as a last resort
 804 in the search for an explanation of the experimental data of thermal blackbody radiation. Five years later,
 805 Einstein introduced the first germ of the idea of quantization of the electromagnetic field, on the basis of
 806 thermodynamic equilibrium of the blackbody "resonators". And Einstein again, in 1916, explained the
 807 relation between stimulated emission and radiation absorption using as well thermodynamic equilibrium
 808 arguments, in a seminal paper that represents the theoretical birthdate of lasers (Einstein (1916)).

809 **Temperature?** Temperature is at the heart of both classical thermodynamics and statistical mechanics,
 810 and yet it is a rather difficult notion to put on firm grounds. The schoolbook definition of temperature
 811 as "average kinetic energy of the system" makes little sense upon closer inspection, unless only the
 812 translational kinetic energy is considered: the amount of energy to increase temperature by 1 degree is
 813 different for a monoatomic vs. a diatomic gas. Kelvin's definition of absolute temperature focused on the
 814 heat exchanges between thermal baths, in the style of Carnot (who in his time did not have the concepts of
 815 heat and entropy, and spoke generally of "caloric"), defining the *ratio* of two temperatures as being equal
 816 to the ratio of the exchanged heat between two bodies. The more formal definition (Gibbs) looks at the
 817 change in entropy as a function of internal energy, at constant- $\{N, V\}$:

$$\frac{1}{T} = \left. \frac{\partial S}{\partial E} \right|_{N,V} \quad (39)$$

818 and defines temperature as an intensive quantity, the ratio between the differentials of two extensive
 819 variables.

820 As we saw in the previous section, defining entropy rigorously for quantum systems with discrete energy
 821 levels is still problematic, and this holds even more true for the notion of temperature. Temperature is a
 822 property of the aggregate system, not of each single particle, and is properly defined only for systems at
 823 equilibrium. Instead, open quantum systems are often found in non-equilibrium states, strongly coupled and
 824 correlated with the environment. Temperature is classically an intensive variable, that is, a physical quantity
 825 that can be measured locally and is the same throughout the system; however, for systems with strong
 826 interactions and a small number of degrees of freedom, locality is lost and some equivalent of temperature
 827 could no longer be found to be intensive (Hartmann and Mahler (2005); García-Saez et al. (2009)). In
 828 standard quantum statistical mechanics, temperature is treated just as a parameter in the wavefunction, and
 829 does not have an operator associated (you usually see it just as the $\beta = 1/k_B T$ relief at the denominator
 830 of the Fermi-Dirac or Bose-Einstein energy exponentials). **A common approach is to assign an effective**
 831 **temperature T^* , as the temperature of an equilibrium Gibbs state with the same average energy, that**
 832 **is $\text{Tr}[H\rho] = \text{Tr}[H(e^{-\beta^* H}/\mathcal{Z})]$ (see Eq.(49) for definitions), under the assumption that after a transient**
 833 **thermalization time, the density ρ will become indistinguishable from the Boltzmann distribution. However,**
 834 **for a quantum system not in equilibrium, just looking at the direction of heat flow is no longer sufficient to**
 835 **define which temperature is the hotter or colder than a reference (thermometer). It has been recently shown**
 836 **experimentally (Micadei et al. (2019)) that in a system made, e.g., of quantum correlated spins prepared at**
 837 **two different local temperatures, heat can flow in reverse from the cold to the hot region. Such a reversal**
 838 **can be explained by a trade-off between the information contained in the correlated state and the reduction**
 839 **of entropy, see e.g. Lloyd (1989); Henao and Serra (2018).**

840 For a quantum system with sufficiently close-spaced energy levels, it is customary to use Von Neumann's
 841 definition, Eq.(27) (which strictly speaking refers to information and not to heat exchanges, Vallejo et al.
 842 (2020)). The reduced density matrix of a qubit in a random point of the Bloch sphere (see Eq.(32)) is then:

$$\rho_r = \frac{1}{2} (1 + \vec{r} \cdot \vec{\sigma}) = \frac{1}{2} \begin{pmatrix} 1 + r_z & r_x - ir_y \\ r_x + ir_y & 1 - r_z \end{pmatrix} \quad (40)$$

843 $\vec{\sigma}$ being the vector with components the Pauli matrices, and the entropy for the modulus $r = |\vec{r}|$ is:

$$\frac{S_r}{k_B} = - \left(\frac{1+r}{2} \right) \ln \left(\frac{1+r}{2} \right) - \left(\frac{1-r}{2} \right) \ln \left(\frac{1-r}{2} \right) \quad (41)$$

844 Let us imagine for the sake of simplicity a spin-qubit μ in a magnetic field \vec{B} , with Hamiltonian
 845 $\mathcal{H} = -2\mu(\vec{r} \cdot \vec{B})$. The internal energy in the density-matrix formalism is defined $E = \langle \mathcal{H} \rangle = \text{Tr}\{\rho_r \mathcal{H}\}$,
 846 from which a quantum equivalent "temperature" follows by formally applying Eq.(39):

$$T = \frac{1}{k_B} \frac{\mu r}{B_{\parallel} \tanh^{-1} r} \quad (42)$$

847 B_{\parallel} indicating the component of \vec{B} projected on \vec{r} . It can be seen that at this level, thermodynamic properties,
 848 and in particular the temperature, are function only of \vec{r} . Note that for pure states on the Bloch surface, the
 849 Von Neumann entropy is zero and such a definition of temperature also goes to zero (with the puzzling
 850 consequence that one could get to absolute zero by using a finite quantity of energy, thus contradicting
 851 the Third Law of thermodynamics). On the other hand, temperature is intended an average quantity that is
 852 applicable only to a system with a large number of degrees of freedom, and in contact with a thermal bath,
 853 that is, in a mixed state.

854 As a next step, let us consider an isolated system of $2N$ non-interacting spin qubits, initially prepared
 855 in an eigenstate with total energy E . At a given temperature, a subset M of spins is excited. For a weak
 856 coupling, it must be $M \ll 2N$. This is a *microcanonical* ensemble that at thermal equilibrium must equally
 857 share the total energy between all its degrees of freedom Ω . To have a density operator that is diagonal in
 858 any base, we must require that the wavefunction is an incoherent superposition of all states with constant
 859 energy E and random phases $\phi_j \in [0, 2\pi]$ (Ghonge and Vural (2018)):

$$|\psi\rangle = \frac{1}{\sqrt{R}} \sum_{j=1}^R e^{i\phi_j} |\psi_M^{(j)}\rangle, \quad R = \binom{2N}{M} \quad (43)$$

860 R is the number of states with M thermally excited spins, and $|\psi_M^{(j)}\rangle$ is the j -th wavefunction of such
 861 ensemble. For example, with $N=4$ and $M=2$, it is $R=28$ and $|\psi_2^{(1)}\rangle=|11000000\rangle$, $|\psi_2^{(2)}\rangle=|10100000\rangle$, ...
 862 $|\psi_2^{(28)}\rangle=|00000011\rangle$. For a given excitation B , the temperature is a function of R :

$$T_R = \frac{1}{k_B} \frac{2\mu B}{\ln(2N/M - 1)} \quad (44)$$

863 An increasing temperature corresponds to an increasing fraction, $M \rightarrow N$, of spins excited; at the
 864 opposite, $T \rightarrow 0$ when the system tends to perfect paramagnetic alignment.

865 **Other concepts of effective temperature have been derived from detailed balance for near-equilibrium**
 866 **conditions (Dann et al. (2020)), for example in the case of the XX-Heisenberg system of two qubits**
 867 **representing an Otto cycle whose energy gaps are changed by the same ratio in the quantum adiabatic**

868 strokes (Huang et al. (2013)). Anyway, the definition of temperature in the quantum regime still remains a
 869 subject of fundamental, and quite "heated" discussions (see, e.g., Kosloff (2013); Hartmann and Mahler
 870 (2005); Ghonge and Vural (2018); Lipka-Bartosik et al. (2023)).

871 **Quantum Carnot.** Classically, the Carnot engine consists of two sets of alternating adiabatic strokes
 872 and isothermal strokes. A priori, one may argue that the laws of thermodynamics (with an exception
 873 for the First) are defined just for macroscopic systems described by statistical averages, and hence, the
 874 question of their validity for microscopic systems consisting of a few particles, or qubits, may itself appear
 875 meaningless. However, already in 1959 (Scovil and Schulz-DuBois (1959)) Scovil demonstrated that
 876 the working of a quantum three-level maser coupled to two thermal reservoirs resembles that of a heat
 877 engine, with an efficiency upper-bounded by the Carnot limit. A quantum analogue of the Carnot engine
 878 consists of a working fluid, which could be a particle in a box (Bender et al. (2000)), qubits of various
 879 kind (Geva and Kosloff (1992)), multiple-level atoms (Quan et al. (2007)) or harmonic oscillators (Lin and
 880 Chen (2003)). For the simplest case of a three-level system, the quantum working fluid is the spectrum
 881 of energy levels $E_1 < E_2 < E_3$; the high-temperature bath can excite transitions $\hbar\omega_h = |E_1 - E_3|$, the
 882 low-temperature sink induces transitions $\hbar\omega_c = |E_1 - E_2|$; and a radiation field is tuned resonantly at
 883 the frequency $\hbar\omega_r = |E_2 - E_3|$. At equilibrium, for each excitation $\hbar\omega_h$ the system loses an energy $\hbar\omega_c$
 884 to the cold sink, and $\hbar\omega_r$ to the radiation, so that the population ratios $n_1/n_3 = \exp(\hbar\omega_h/k_B T_h)$ and
 885 $n_1/n_2 = \exp(\hbar\omega_c/k_B T_c)$ are maintained steady. The energy exchanged with the two thermal baths can
 886 be thought of as "heat" (positive or negative), while the energy exchanged with the radiation field can be
 887 identified with "work" extracted from the quantum system (the radiation plays the same role as Carnot's
 888 "piston"). This identification of work and heat implies the energy relation $\hbar\omega_h = \hbar\omega_c + \hbar\omega_r$, which is the
 889 analog of entropy conservation for a reversible cycle. (Reversibility here is within the limit of statistical
 890 equilibrium among all the excitations.)

891 A remarkable result appears when the efficiency of this "thermodynamic" system is considered. The
 892 quantum system can work as an engine when a population inversion is realized between the levels 2 and 3,
 893 $n_3 > n_2$, which leads to a condition:

$$\frac{n_3}{n_2} = \frac{n_3 n_1}{n_1 n_2} > 1 = \exp\left(\frac{\hbar\omega_c}{k_B T_c} - \frac{\hbar\omega_h}{k_B T_h}\right) \geq 1 \quad (45)$$

894 The efficiency is, as usual, the ratio of the work extracted to the heat supplied by the hot reservoir,

$$\eta = \frac{\hbar\omega_r}{\hbar\omega_h} = 1 - \frac{\hbar\omega_c}{\hbar\omega_h} \quad (46)$$

895 which - thanks to the previous inequality - gives Carnot's limit $\eta \leq 1 - T_c/T_h$.

896 The proof of existence of Carnot's limit (a manifestation of the Second law of thermodynamics) at
 897 quantum length scales establishes a strong case for the emergence of thermodynamic laws at the most
 898 fundamental level. Quantum cyclic processes, although different in many ways from a Carnot cycle, still
 899 have important features in common with it. Most importantly, however, it has been shown that a quantum
 900 engine could exceed the capabilities of the Carnot cycle, in that it can operate between reservoirs of positive
 901 and negative temperatures (Geusic et al. (1967)).

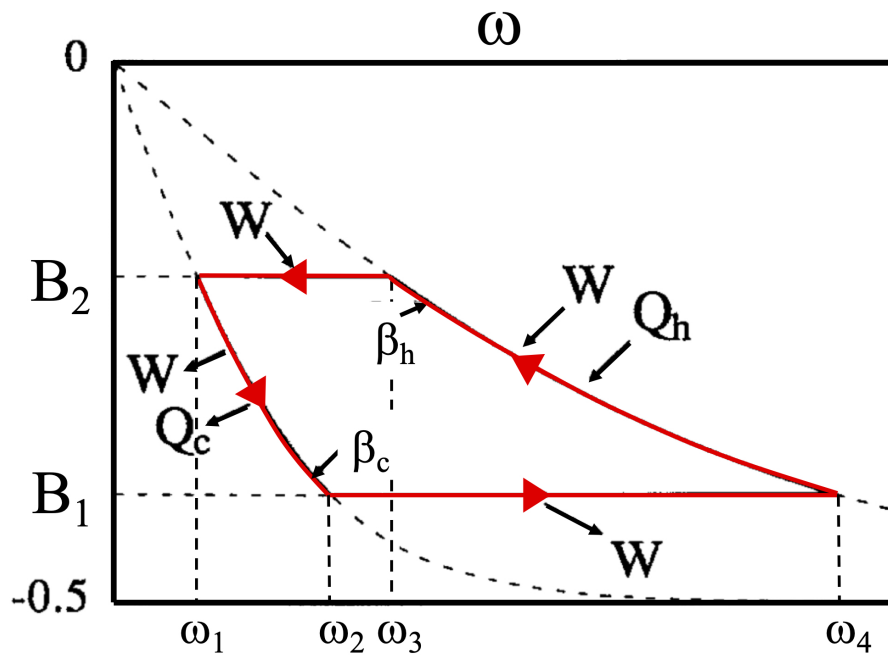


Figure 4. A reversible quantum Carnot cycle depicted in the space of the normalized magnetic field ω and the magnetization B . The horizontal lines represent adiabats wherein the engine is uncoupled from the heat baths at inverse temperatures $\beta_{h,c} = 1/k_B T_{h,c}$, and the magnetic field is changed between two values; the two horizontal strokes represent changing the magnetisation ω while the qubits are connected to a heat bath at constant temperature. Black arrows indicate the direction of heat and work from/to the spin-qubit system. (Adapted w. perm. from Ref.[58]).

902 The classical definition Eq.(39) of temperature as the variation of entropy with energy, allows in theory
 903 a negative value of temperature if for some system the entropy does not increase, but rather decreases
 904 upon increasing energy. The conditions by which this could happen were first identified by Onsager
 905 (Onsager (1949)), and more precisely stated by Ramsey, as far back as 1956 (Ramsey (1956)). The
 906 simplest example is a 1D chain of 1/2-spins of non-interacting qubits with gyromagnetic constant γ , in a
 907 magnetic field $\omega(t) = -\gamma B_z(t)$ (Geva and Kosloff (1992)). The time-dependent Hamiltonian is simply
 908 $\mathcal{H}(t) = \hbar\omega(t)\sigma_z/2$, coupled to two baths at temperatures T_h and T_c (Figure 4). During the adiabatic
 909 expansion, $\omega_2 \rightarrow \omega_4$, and compression, $\omega_3 \rightarrow \omega_1$, work is done by, or on the spins, but entropy is constant;
 910 in the cold, $\omega_1 \rightarrow \omega_2$, and hot isotherm, $\omega_4 \rightarrow \omega_3$, both heat and work are transferred to the cold bath, or
 911 removed from the hot bath, while entropy, respectively, decreases or increases. The expectation value of
 912 the Hamiltonian is obtained as:

$$\frac{d\langle\mathcal{H}(t)\rangle}{dt} = \frac{1}{2} \left(\frac{d\omega}{dt} \langle\sigma_z\rangle + \omega \frac{d\langle\sigma_z\rangle}{dt} \right) \tag{47}$$

913 The two terms on the RHS are to be identified, respectively, with the average work, $\langle\delta W\rangle = \langle\sigma_z\rangle\delta\omega/2$,

914 and average heat, $\langle\delta Q\rangle = \omega\delta\langle\sigma_z\rangle/2$, exchanged, in the analog of the derivation of the First Law (see
 915 Eq.(50) below).

916 Now, consider the extreme situation in which the total magnetic energy of the spin chain increases
917 continuously from the lowest state with all spins "down", up to the highest state with all spins "up". Both
918 the initial and final states have just one microstate available, $\Omega=1$ $p_1=1$, therefore their Von Neumann
919 entropy is zero. While the magnetic field spans between these two extremes, the entropy first increases
920 from 0, goes to its maximum when the spins are on average half-up and half-down, and then decreases
921 again going back to 0. Correspondingly, the temperature goes from zero to plus-infinity at the entropy
922 maximum, then jumps to negative-infinity (because entropy and energy have opposite-sign first derivatives)
923 and goes back to zero always from negative values.

924 As Ramsey pointed out (Ramsey (1956)), the number of physical systems actually capable of assuming a
925 negative temperature is limited to systems with a finite number of energy levels, and sufficient thermal
926 insulation from positive-temperature reservoirs. In the real-world, atomic or nuclear spin systems have other
927 degrees of freedom; if the coupling between the spins and other degrees of freedom is much weaker than
928 the strong coupling between spins, we can talk about a "spin-temperature" separately from the temperature
929 of the atoms, or lattice as a whole. It is interesting to note that if one can realize a system simultaneously
930 coupled to a positive and a negative thermal bath, Carnot's efficiency $(1 - T_1/T_2)$ could indeed assume
931 values larger than 1 (Geusic et al. (1967)).

932 By using quantum mechanical states as the heat exchanger "fluid", even a single atom can turn into
933 a Carnot engine, as shown by Singer's group in Mainz (Rosnagel et al. (2016)). Sandwiched between
934 an electric field representing the hot reservoir and a laser cooling beam representing the cold reservoir,
935 a single $^{40}\text{Ca}^+$ ion is caught in a funnel-shaped, magnetic quadrupole linear trap, with frequency ω_r .
936 The "temperature" of the ion quantum state is determined by the radial spreading of the wavefunction,
937 approximately Gaussian with a width $\sigma(T) = (k_B T / m \omega_r^2)^{1/2}$. The cooling laser is always on, while the
938 electric field switched on and off, thereby making the ion temperature oscillate between "cold" and "hot";
939 by sweeping the trap frequency between the extremes $\pm\omega_M$, a thermodynamic cycle is performed and work
940 is extracted by the axial force generated by the movement of the trapped ion. Compared to the equivalent
941 Carnot cycle, the efficiency is extremely small, of the order of 0.003, however the result of a single ion
942 performing as a reversible and essentially frictionless quantum engine is nothing short of amazing.

943 The same group had previously demonstrated (but not experimentally realized, at least yet) an example
944 of a Otto cycle for a time-dependent oscillator coupled to a "squeezed" thermal reservoir, which could
945 have a theoretical efficiency above Carnot's limit and approaching unity (Rosnagel et al. (2014)). There,
946 the squeezing (a common concept in quantum optics, (Breitenbach et al. (1997))) refers to the particular
947 construction of the quantum states of the thermal bath, in which the thermal noise is distributed differently
948 among the degrees of freedom; for example, in a harmonic oscillator the noise can be concentrated in the
949 phase but not in the amplitude (Breitenbach et al. (1997); Esteve et al. (2008)).

950 **Thermal vs. quantum fluctuations.** Thermodynamics is a macroscopic effective picture of thermal
951 processes, not concerned with microscopic details, but only dealing with average quantities such as
952 temperature, work, dissipated heat. **This classical approach is valid for a macroscopic number of particles
953 in the so-called thermodynamic limit ($N \rightarrow \infty, V \rightarrow \infty$, with $N/V = \text{const}$), but starts losing accuracy
954 as the system size decreases to a small number of degrees of freedom. In this regime, thermal fluctuations
955 of the average quantities can become as relevant as the averages themselves, or more, since they alone may
956 induce deviations from the average behavior (Alemany and Ritort (2010)).** Compared with macroscopic
957 thermodynamics, fluctuations play a much more important role in small systems. However, the presence
958 of fluctuations does not mean that we cannot characterize quantum systems thermodynamically; on the

959 contrary, fluctuations typically contain important additional thermodynamic and energetic information that
960 is usually lost as noise in the infinite-system limit.

961 Stochastic thermodynamics picks up where the macroscopic description starts to fail, and gives insight into
962 the fluctuations of thermodynamic quantities. It also moves beyond the equilibrium situations associated
963 with thermodynamics, and can describe the behavior of systems that are out of equilibrium. Considerations
964 stemming from fluctuation theorems (Evans et al. (1993); Jarzynski (1997); Crooks (1999)) are vital
965 when considering nanoscale devices, or biological protein machines, for which experiments confirmed
966 the theoretical predictions of local violation of the Second Law (Wang et al. (2004)). Such "theorems"
967 (in fact, they should be better called "relations", since they do not stem from a rigorous derivation from
968 a set of axioms) state at different levels that for dynamical systems far from equilibrium there exists a
969 physically meaningful, real-valued variable Ω_t , extensive both in space and time, whose positive values are
970 exponentially more probable than the negative ones, or:

$$\frac{P(+\Omega_t)}{P(-\Omega_t)} = e^{\Omega_t} \quad (48)$$

971 In practice, this variable is easily identified with the entropy production, extensive and increasing with
972 time. What such fluctuation relations state, therefore, is that the Second Law probabilistically holds for a
973 macroscopic system observed over macroscopic times. And it can be "violated" (that is, entropy flows in
974 the reverse direction) if the system is sufficiently small and/or the observation time is sufficiently short. In
975 particular, according to Crook's fluctuation relation (Crooks (1999)), for a transformation between two
976 microscopic states A and B separated by a free energy ΔF , the thermodynamic work W is a fluctuating
977 quantity, and is therefore given by a probability distribution of values. For ideally reversible transformations,
978 the work distributions in the time-forward or backward direction cross at the value $W = \Delta F$, as clearly
979 demonstrated by optical tweezers experiments on the cyclic folding and unfolding of RNA fragments
980 (Collin et al. (2005)).

981 At the even smaller scale, however, fluctuations are no longer just thermal, but quantum-mechanical in
982 origin. In the regime in which quantum phenomena are manifest, that is, very low temperatures and sizes
983 smaller than the De Broglie wavelength, Heisenberg's uncertainty relations become the relevant source of
984 noise in the form of localized, temporary random changes of the system energy, for a (very) short time.
985 Then, many questions arise when applying such concepts to qubits. For example:

- 986 • What becomes of thermodynamic equilibrium, for time-reversible, unitary transformations?
- 987 • What is the meaning of thermalization in the presence of quantum integrals of motion?
- 988 • How to define and/or measure thermodynamic quantities for quantum systems?
- 989 • How entanglement is connected with the information entropy?
- 990 • and more...

991 The fluctuations we are after for a quantum system in contact with a heat bath are not strictly thermal
992 ones. Rather, they are represented by combinations of (1) the possible changes in the distributions of the
993 energy levels (that is, a change of the Hamiltonian), and/or (2) changes of their occupation numbers (that
994 is, entropy). In both cases, the result is a degradation of the quantum state, i.e. a loss of coherence. The
995 pure state turns into a mixed state.

996 In the approximation of weak coupling between the quantum system and the thermal bath, the equilibrium
 997 density tends to a Gibbs state ($\beta = 1/k_b T$):

$$\rho^{eq} = \frac{\exp(-\beta\mathcal{H})}{\mathcal{Z}} \quad (49)$$

998 with as usual $\mathcal{Z} = \text{Tr}\{\exp(-\beta\mathcal{H})\}$ the system's partition function. The average internal energy is $E(\rho) =$
 999 $\text{Tr}\{\mathcal{H}\rho\}$, the entropy $S = -\text{Tr}\{\rho \ln \rho\}$, and the free energy is obtained as $F = E(\rho) - TS(\rho) = -\ln \mathcal{Z}/\beta$.
 1000 Hence, a "weak" quantum-equivalent of the First Law can be written:

$$dE = \delta Q + \delta W = \text{Tr}\{(d\rho^{eq})\mathcal{H}\} + \text{Tr}\{\rho^{eq}(d\mathcal{H})\} \quad (50)$$

1001 The first term on the right-hand side, containing the differential of the equilibrium density, is relative
 1002 to a variation of occupation numbers of the quantum eigenstates, and is therefore assimilated to a form
 1003 of thermodynamic entropy analogous to the δQ of classical thermodynamics; the second term, in turn,
 1004 containing the differential of the system Hamiltonian, corresponds to a change in the structure of the energy
 1005 levels, as it could derive by a change in the system mechanics, and can be assimilated to a work δW done
 1006 on, or by, the quantum system.

1007 **Work and heat are not quantum-mechanical observables.** Both quantities are dependent on the process
 1008 path λ (and thus are non-exact differentials, like in classical thermodynamics), which means they do
 1009 not correspond to quantum-mechanical observables, i.e. there is no Hermitian operator \hat{q} or \hat{w} such that
 1010 $Q = \text{Tr}\{\rho\hat{q}\}$ and $W = \text{Tr}\{\rho\hat{w}\}$. The intuitive, simplistic reasoning behind such a statement is that the
 1011 final-state Hamiltonian at $t=\tau$ does not necessarily commute with the initial Hamiltonian at $t=0$, i.e.

$$[\mathcal{H}(\lambda^t), \mathcal{H}(\lambda^\tau)] \neq 0 \quad (51)$$

1012 for some (or all) times $0 < t < \tau$.

1013 A different definition of *quantum work* (w/r to Eq.(50)) can be given as the difference between eigenvalues
 1014 of the "instantaneous" Hamiltonian at the beginning and end of the path λ :

$$W = \left(\epsilon_m^{\lambda\tau} - \epsilon_n^{\lambda 0} \right) \quad (52)$$

1015 Here quantum work is a random variable distributed as $p(W; \lambda)$, and is given by a time-ordered correlation
 1016 function as a path-dependent quantity. On this basis, the quantum-equivalent of the fluctuation theorems
 1017 can also be recovered (Talkner et al. (2007); Hänggi and Talkner (2011)):

$$\frac{p(W; \lambda)}{p(-W; \lambda)} = e^{\beta(W - \Delta F)} \quad (\text{Crooks}) \quad (53)$$

$$\langle e^{\beta W} \rangle_{\lambda} = e^{-\beta \Delta F} \quad (\text{Jarzinsky}) \quad (54)$$

1018 However, for a quantum system entangled with its environment the interaction energies are not weak, in
 1019 fact they will quickly degrade the pure state into a mixed one, in a time of the order of the coherence time.
 1020 Identification of "heat" and "work" with the variation of the system's characteristics ($d\rho, d\mathcal{H}$) is no longer
 1021 enough. During isothermal quasi-static processes, part of the free energy exchanged with the environment
 1022 represents an "energetic price" to pay, in order to preserve the coherence and quantum correlations in the
 1023 system. Denoting a non-Gibbsian, *coherent* and *correlated* state as ρ^{cc} , the extended entropy S_e can be
 1024 written as :

$$\begin{aligned} S_e &= -\text{Tr}\{\rho^{cc} \ln \rho^{cc}\} = \\ &= -\text{Tr}\{\rho^{cc} \ln \rho^{cc}\} + [\text{Tr}\{\rho^{cc} \ln \rho^{eq}\} - \text{Tr}\{\rho^{cc} \ln \rho^{eq}\}] = \\ &= \beta[E - (F + TS(\rho^{cc}||\rho^{eq}))] = \beta[E - \mathcal{F}] \end{aligned} \quad (55)$$

1025 (note that the last term in [...] in the second line is zero). $S(\rho^{cc}||\rho^{eq}) = \text{Tr}\{\rho^{cc}(\ln \rho^{cc} - \ln \rho^{eq})\}$ is
 1026 the quantum relative entropy (Vedral (2002)), and $\mathcal{F} = F + TS(\rho^{cc}||\rho^{eq})$ is the so-called information
 1027 free energy (Parrondo et al. (2015)). In analogy with the perfect-Gibbs case, consider the non-Gibbsian
 1028 infinitesimal of dS_e :

$$\begin{aligned} dS_e &= \beta(dE - d\mathcal{F}) = \beta(\text{Tr}\{(d\rho^{cc})\mathcal{H}\} + \text{Tr}\{\rho^{cc}(d\mathcal{H})\} - d\mathcal{F}) \\ &\equiv \beta(\delta Q_{tot} - \delta Q_{cc}) \end{aligned} \quad (56)$$

1029 where $\delta Q_{tot} = \text{Tr}\{(d\rho^{cc})\mathcal{H}\}$ is assimilated to the total heat exchanged, and $\delta Q_{cc} = d\mathcal{F} - \text{Tr}\{\rho^{cc}(d\mathcal{H})\}$
 1030 is the "energetic price" to maintain coherence and correlation.

1031 Then, the "entangled system" quantum-equivalent of the First Law can now be written as:

$$de = dS_e/\beta + \delta\mathcal{F} = \text{Tr}\{(d\rho^{cc})\mathcal{H}\} + \text{Tr}\{\rho^{cc}(d\mathcal{H})\} \quad (57)$$

1032 only formally similar to the previous statement, Eq.(50), but with the peculiarly different meaning of the
 1033 symbols for E, S_e, \mathcal{F} .

1034 **Quantum version of Landauer's limit.** Consider a quantum system S whose information content is
 1035 progressively erased upon interacting with a quantum environment E . Both S and E are living in their
 1036 respective Hilbert spaces $\mathcal{W}_S, \mathcal{W}_E$. Assume that the initial state of the composite system is factorized

$$\rho_{SE}(0) = \rho_S(0) \otimes \rho_E(0) \quad (58)$$

1037 such that no initial correlations are present. The environment is initially prepared in a thermal Gibbs state

1038 $\rho_E(0) = \exp(-\beta\mathcal{H}_E)/\mathcal{Z}_E$. S and E interact via the unitary transformation $U(t) = \exp(-i\mathcal{H}t/\hbar)$, with
 1039 $\mathcal{H} = \mathcal{H}_S + \mathcal{H}_E + \mathcal{H}_{SE}$ the total Hamiltonian comprising the system, the environment and their interaction.

1040 Landauer's principle is related to the change in entropy of the total system plus environment, therefore
 1041 we can reinterpret the heat exchanged between S and E , as the difference between their respective initial
 1042 and final entropy:

$$[S(\rho_S^t) - S(\rho_S^0)] + [S(\rho_E^t) - S(\rho_E^0)] = \Delta S_S - \Delta S_E = \mathcal{I}(\rho_{SE}^t) \geq 0 \quad (59)$$

1043 This is, by definition, also equal to the *quantum mutual information* exchanged between S and E :

$$\mathcal{I}(\rho_{SE}^t) = S(\rho_E^t) + S(\rho_S^t) - S(\rho_{SE}^t) \quad (60)$$

1044 (Note that for a completely factorized initial state, $\mathcal{I}(\rho_{SE}^0) = 0$.) With some algebra (see full derivation

1045 in Ref. Reeb and Wolf (2014)) it is shown that the average heat dumped from S into the environment,
 1046 $\langle Q_E \rangle = \text{Tr}\{(\rho_E^t - \rho_E^0)\mathcal{H}_E\}$, is equal to:

$$\beta\langle Q_E \rangle = \Delta S_S + \mathcal{I}(\rho_{SE}^t) + S(\rho_E^t || \rho_E^0) \quad (61)$$

1047 And since both $\mathcal{I}(\rho_{SE}^t)$ and $S(\rho_E^t || \rho_E^0) \geq 0$, it is also:

$$\beta\langle Q_E \rangle \geq \Delta S_S \quad (62)$$

1048 This important relationship therefore establishes that the only heat dissipation in quantum computing

1049 occurs during state initialization and reset (erasure) operations, which are both linear in the number of
 1050 qubits: the entropy changes in the quantum system turn into heating of the environment, by an amount
 1051 simply proportional to the number of qubits, and not to the dimension of their Hilbert space. That's quite
 1052 good news, since for N qubits the Hilbert space has dimension 2^N or, in other words, 2^N -distinct possible
 1053 eigenstates, a number that grows very quickly. A classical computer simulating this quantum computer,
 1054 instead, must use an energy at least equal to $2^N k_B T \ln 2$ just to initialize or erase the configuration. Hence,
 1055 this represents an additional bound to quantum advantage for a given classical calculation.

1056 Equation (62) has been verified experimentally in a number of cases. In Figure 5 the results of two such
 1057 experiments are reported (Yan et al. (2018); Cimini et al. (2020)).

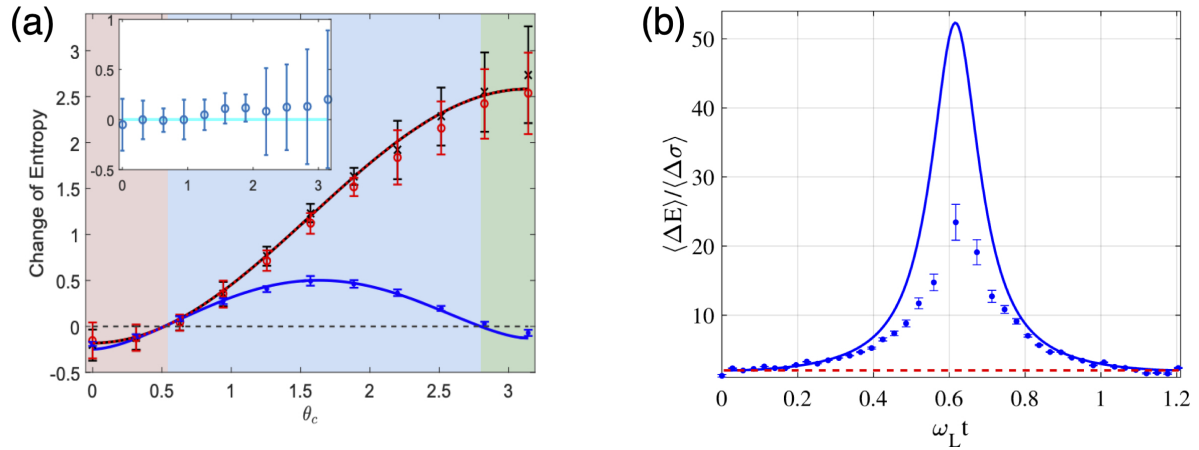


Figure 5. (a) Experimental verification of Eq.(62) on a ^{40}Ca ion-trap qubit. Black data = $\beta\langle Q_E \rangle$; red data = $\Delta S_S + \mathcal{I}(\rho_{SE}^t) + S(\rho_E^t || \rho_E^0)$ (reprinted w. perm. from Ref. Yan et al. (2018)). (b) The $\beta\langle Q_E \rangle \geq \Delta S_S$ limit demonstrated experimentally on a toy-model optical qubit gate. (Reprinted w/perm. from Ref.[34]).

1058 **Thermalization: randomization of pure states into mixed states.** The typical initial condition of a
 1059 quantum computer is a *pure state*, for example with all the qubits prepared in a same state $|\psi_i\rangle = \begin{pmatrix} 1 \\ 0 \end{pmatrix}$ for
 1060 $i \in N$, by a previous RESET operation. As we saw in the subsection above, this operation costs both energy
 1061 and heat, but it is fortunately linear with N . Quantum decoherence explains how a system interacting with
 1062 an environment, transitions from being a pure state (which exhibits coherent superpositions) to a mixed
 1063 state, that is an incoherent combination of classical alternatives. The transition is ideally reversible, as the
 1064 combined state of system and environment may still be a pure state. However, for all practical purposes it
 1065 should be seen as irreversible, as the environment is in general a very large and complex quantum system,
 1066 and it is not practically feasible to reverse their interaction.

1067 A general description of the transformations between states when the quantum system is interacting
 1068 with an external environment can be given by a kind of master equations, first introduced by Lindblad
 1069 (Lindblad (1976)). Such dynamics preserves trace and positivity of the density matrix, while allowing the
 1070 density matrix to vary otherwise (Breuer and Petruccione (2002)). Master equations have the general form
 1071 (Manzano (2020)):

$$\frac{d\rho}{dt} = -\frac{i}{\hbar} [\mathcal{H}, \rho] + \sum_k \left[L_k \rho L_k^\dagger - \frac{1}{2} (L_k^\dagger L_k \rho + \rho L_k L_k^\dagger) \right] \quad (63)$$

1072 (to be compared with Eq.(33) above). The L_k are Lindblad operators that describe the effect of the
 1073 interaction between the system and the environment on the system's state. A good example is the interaction
 1074 of the 1/2-spin qubit with an electromagnetic field, for which there is just one operator $L = \sigma^+$, $L^\dagger = \sigma^-$,
 1075 which applied on the qubit give $\sigma^- |0\rangle = |1\rangle$ and $\sigma^+ |1\rangle = |0\rangle$. The external photon field is described by a
 1076 spontaneous emission rate γ_0 , with number density N given by the Bose-Einstein distribution:

$$N = \frac{1}{e^{\beta\omega} - 1} \quad (64)$$

1077 and $\gamma = \gamma_0(2N + 1)$ is the total emission rate, including thermally-induced absorption and emission at the

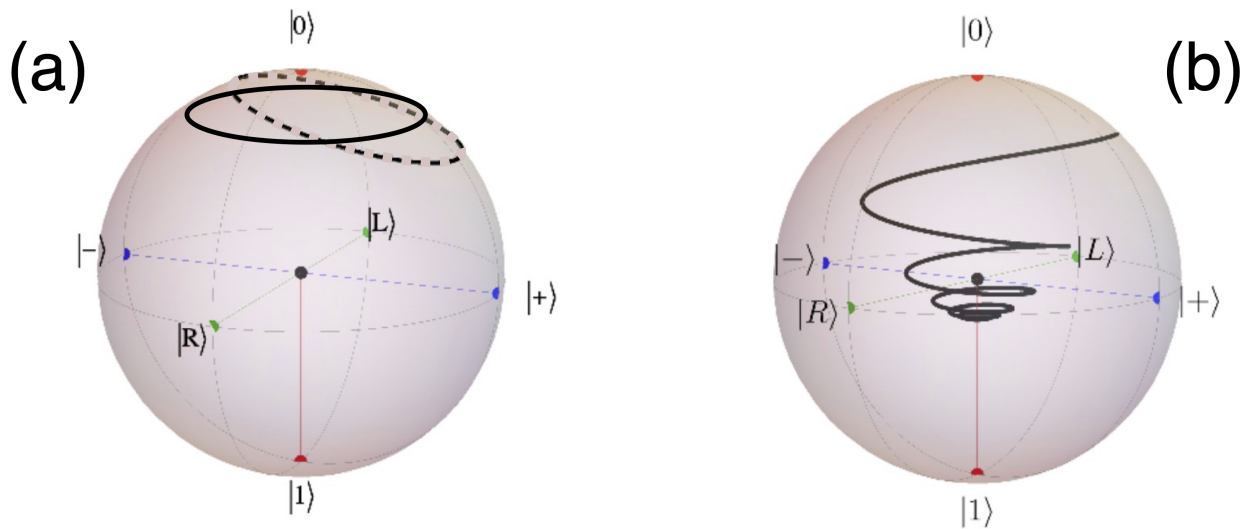


Figure 6. (a) Unitary dynamics from Eq.(33), and (b) dissipative dynamics from Eq.(65) in the Bloch sphere. (Adapted from G.T. Landi, w/perm.)

1078 temperature $\beta = 1/k_B T$ (Cherian et al. (2019); Jäger et al. (2022)). The master equation describing the
 1079 evolution is:

$$\frac{d\rho}{dt} = -\frac{i}{\hbar} [\mathcal{H}, \rho] + \gamma_0(N+1)\mathcal{D}(\sigma^-) + \gamma_0 N \mathcal{D}(\sigma^+) \quad (65)$$

1080 where the more compact "dissipator" notation $\mathcal{D}(L) = L\rho L^\dagger - \frac{1}{2}\{L^\dagger L, \rho\}$ has been introduced. Figure
 1081 6a,b compares the evolution of the density matrix $\rho(t)$ in the two cases: (a) under the action of Eq.(33),
 1082 with the unitary Hamiltonian $\mathcal{H}_0 = \hbar\omega\sigma_z/2$, and (b) the dissipative Eq.(65). All the unitary Hamiltonian
 1083 does is a precession of the state vector around z ; on the other hand, upon coupling to the dissipator operator
 1084 the precession is accompanied by a damping towards the z -axis. (Side note: The Hamiltonian for a spin
 1085 population pumped by a coherent laser source, $\mathcal{H} = \mathcal{H}_0 + \frac{\lambda}{2}(\sigma^+ + \sigma^-)$, is still unitary and hermitian (the
 1086 rates of upward and downward transitions are equal), the result is just a precession about an axis inclined
 1087 w/r to z , see dashed line in Fig.6a.)

1088 It is worth noting that the time-independent generator in Lindblad form describes a *memoryless* dynamics
 1089 of the open system, typically leading to an irreversible loss of characteristic quantum features. However, in
 1090 many applications open systems exhibit pronounced memory effects, in the more general framework of
 1091 non-Markovian quantum dynamics (Breuer et al. (2016)). Typically, this is due to the fact that the relevant
 1092 environmental correlation times are not small compared to the system's relaxation or decoherence time,
 1093 thus rendering the standard Markov approximation not applicable. The violation of this separation of time
 1094 scales can occur, for example, in the cases of strong system-environment couplings, structured or finite
 1095 reservoirs, low temperatures, or large initial system-environment correlations (see, e.g., Verstraete et al.
 1096 (2009); Hanson et al. (2008); Zhang et al. (2017); Shen et al. (2013)).

1097 Decoherence describes the classical limit of quantum mechanics, but is different from wavefunction
 1098 collapse. In the mixed state all classical alternatives are still present, whereas the wavefunction collapse

1099 (i.e., a measurement) selects only one of them (Hill and Wootters (1997); Wootters (1998)). Consider two
 1100 qubits A and B (e.g., spin-1/2 particles, or polarized photons) characterized by an excitation energy E , at a
 1101 temperature $k_B T = 1/\beta$, so that the thermal probability of the excited state is $p = [1 + \exp(-\beta E)]^{-1}$.
 1102 Both a pure and a mixed state can be entangled over the ensemble of their qubits, however the difference
 1103 between the two cases is important. A pure state is called entangled when it is unfactorizable. One of
 1104 the simplest definitions of entanglement of a pure state can be given as the (Von Neumann) entropy of
 1105 either member of the pair. A mixed state, on the other hand, is called entangled if it cannot be represented
 1106 as a mixture of factorizable pure states. The entanglement of a mixed state ρ is the minimum average
 1107 entanglement of an ensemble of pure states that represents ρ .

1108 The entanglement of formation $\epsilon_f(\rho)$ of the mixed state ρ , is the quantity of resources needed to create
 1109 a given entangled state. Bennett et al. (1996) $\epsilon_f(\rho)$ is defined as the average entanglement between pure
 1110 states of the decomposition, minimized over all the decompositions ψ_i of ρ (Verstraete et al. (2001)):

$$\epsilon_f(\rho) = \min \sum_i p_i S(\psi_i) = S_e \left[\frac{1}{2} \left(1 + \sqrt{1 - C} \right) \right] \quad (66)$$

1111 also related to a different measure of entanglement, the *concurrence* $C(\rho)$, via the Shannon entropy S_e .

1112 In a quantum computation, maximally-entangled states of a pair of qubits (Bell states) can be constructed
 1113 as we saw in Section 3 above, by applying a Hadamard gate (rotation) followed by a CNOT; let us call
 1114 these two unitary operators U_1 and U_2 . Starting from an initial density ρ_i , the final maximally entangled
 1115 state is $\rho_f = U_2 U_1 \rho_i U_1^\dagger U_2^\dagger$ (Verstraete et al. (2001)). What is interesting to note here, is that after some
 1116 algebra, the concurrence of the final state can be obtained explicitly as:

$$C = \max \left(0, 2p^2 - p - 2(p-1)\sqrt{p(1-p)} \right) \quad (67)$$

1117 This suggests the existence of an "entanglement threshold": for $p \lesssim 0.698$, or equivalently for $k_B T/E \gtrsim$
 1118 1.19, no entangled state of two qubits can be produced. For the typical TransMon excitation energy of the
 1119 order of $E=4$ GHz, the maximum entanglement temperature is $T \simeq 240$ mK. Note that this limit is well
 1120 above the working temperature of SC loops, around 10-20 mK, while trapped ion qubits are operated at
 1121 even lower, liquid-He temperatures.

1122 **Many qubits, multipartite systems.** We can associate to every unitary operation U a work cost $W =$
 1123 $\text{Tr } \mathcal{H}(\rho^f - \rho^i)$, which corresponds to the external energy input required to perform that operation. Think
 1124 of two qubits A and B in a same thermal state at a temperature $T = 1/\beta$; their initial thermal state is joint,
 1125 we can write $\rho_{AB}(\beta) = \rho_A(\beta) \otimes \rho_B(\beta)$, but their Hamiltonian is non-interacting, $\mathcal{H}_{AB} = \mathcal{H}_A + \mathcal{H}_B$.
 1126 To entangle (correlate) them we must bring the joint system out of equilibrium. Necessarily $W > 0$ for
 1127 every possible U because the initial state is in thermal equilibrium. Then, a relevant question is: what is
 1128 the minimal work cost for correlating thermal states? Or equivalently, what is the maximal amount of
 1129 attainable correlations when the energy at our disposal is necessarily limited?

1130 The result of a limiting temperature for the entanglement of a pair of qubits, obtained from Eq.(67), can
 1131 be generalized to the case of multiple qubits (Huber et al. (2015)). Consider N qubits and the rotation
 1132 (Hadamard) from a pure to a maximally-entangled state in the subspace $|0\rangle^{\otimes N}, |1\rangle^{\otimes N}$. Next, consider the

1133 possible bipartitions of the system ($j|N - j$), for which we consider a subpart of the system of $j < N$
 1134 qubits entangled with its complement $N - j$. It has been shown that the concurrence is in fact independent
 1135 on the particular choice of the bipartition, and depends only on the system size:

$$C = p^N - (1 - p)^N - 2p^{N/2}(1 - p)^{N/2} \quad (68)$$

1136 Again, we ask what is the smallest thermal factor $p_b = [1 + \exp(-E/k_B T_b)]^{-1}$, or the maximum
 1137 temperature $k_B T_b = 1/\beta_b$, which allows to simultaneously obtain entanglement across all the possible
 1138 bipartitions of the system. By imposing C to be positive, that is:

$$\frac{1}{\beta_b E} \geq \frac{N}{2 \ln(1 + \sqrt{2})} \quad (69)$$

1139 The corresponding work of correlation for the maximally-entangled set is:

$$W = NE \frac{(1 - e^{-N\beta_b E})}{2(1 + e^{-\beta_b E})^N} = NE \frac{1 + \sqrt{2}}{[(1 + \sqrt{2})^{2/N} + 1]^N} \quad (70)$$

1140 which is exponentially small in the number of qubits N . This interesting result proves that by increasing
 1141 the number of qubits, it becomes possible to generate partial entanglement even at (arbitrarily) high
 1142 temperatures. This is due to the fact that typical gate protocols act on qubit subspaces, whose population
 1143 becomes negligible in the limit of large N . Therefore, even a small amount of entanglement obtained on a
 1144 subset of the available states might be enough to obtain a substantial quantum advantage.

1145 How many correlations can be induced in a system of many qubits? And how can we make sure that a set
 1146 of qubits is actually entangled? This is the more general problem of entanglement detection. Guhne and
 1147 Toth (2009) A measure of the total number of correlations gives the deviation of the global state of the
 1148 quantum computer from a corresponding uncorrelated state, a quantity that is important to estimate in the
 1149 preparation of the initial correlated state. The total system composed of k subsystems would be said to
 1150 have zero correlation if its state is such that $\rho = \otimes \rho_i, i \in k$, i.e. the direct product of its partials. Therefore,
 1151 a common measure of the correlation can be given by the relative entropy of the state (Goold et al. (2016);
 1152 Bennett et al. (2011); Girolami et al. (2017)):

$$S_{rel}(\rho) = \sum_i S_i(\rho_i) - S(\rho) \quad (71)$$

1153 Despite its apparent simplicity, such a measure is highly non-linear and difficult to access in a real
 1154 experimental device with more than just a few qubits, so that alternative approaches have been proposed,
 1155 based e.g. on the Rényi entropy (Brydges et al. (2019)), or the measurement of "witness" observables
 1156 (Guhne and Toth (2009); Friis et al. (2019)), or more general quantifiers including the notion of "fidelity"
 1157 (Liang et al. (2019); Liu et al. (2022)).

1158 **The supremacy clause of thermodynamics.** As it was briefly discussed in Section 4, the fundamental
 1159 noise limit for classical computers is of thermal origin, with a contribution $\mathcal{O}(k_B T)$. To prevent random
 1160 bit flipping, the excitation energy E needs to be sufficiently larger than the thermal energy $k_B T$. Under
 1161 reasonable assumptions, the error probability in assigning a state to a classical bit is (Kish (2002)):

$$\epsilon_Q \gtrsim \exp(-E/k_B T) \tag{72}$$

1162 For a quantum computer with gates driven by auxiliary oscillators at frequency ω (with $\omega > 2\pi/\tau$, and τ
 1163 the coherence time), the corresponding lower error limit is (Gea-Banacloche (2002b)):

$$\epsilon_Q \gtrsim \frac{\hbar\omega}{E} > \frac{h}{E\tau} \tag{73}$$

1164 It can be noted that this is a sort of generalized time-energy uncertainty relation, describing the minimum
 1165 energy needed to change a state in a time less than τ with failure probability smaller than ϵ_Q . The meaning
 1166 of this comparison is that in the quantum case the error decreases only in inverse proportion as the energy
 1167 used, while in the classical case it decreases exponentially. The quantum regime corresponds to $\hbar\omega > k_B T$,
 1168 that is when the quantum noise in the driving oscillator exceeds the thermal noise at the work temperature.

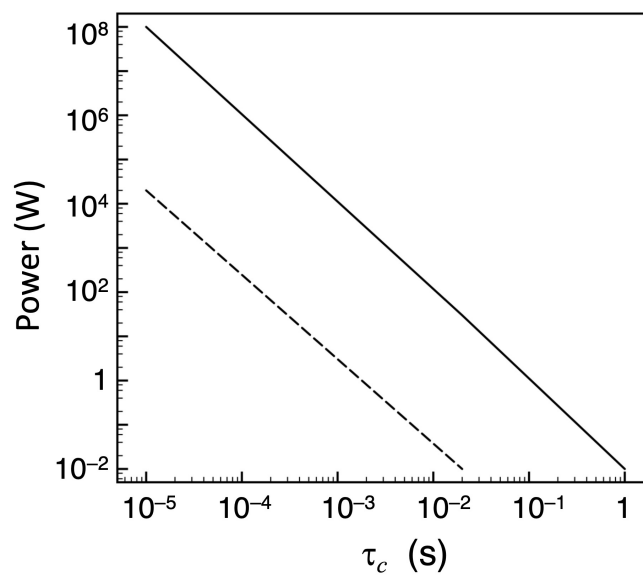


Figure 7. Estimate of minimum power required to factor a 1000-bit number, as described in the text. Solid line: oscillatory control fields, $\omega = (\epsilon_Q^{3/2} \tau)^{-1}$. Dashed line: static control fields only. (Reprinted w/perm. from Ref.[55])

1169 Because of quantum reversibility the excitation energy E need not be dissipated, it only needs to be put
 1170 into, and removed from, the driving system to switch on and off the desired gate evolution. In theory, if
 1171 nothing is ever erased, “conservative” computation is possible. However, there are two caveats. Firstly, any
 1172 proposed quantum computer architecture up to date has no mechanisms to actually “recycle” that energy.
 1173 Current SC gates are based on microwave power pulses, which obviously consume energy irreversibly.

1174 However, any practical computer, even if it could use fully-reversible gates, is still going to generate heat at
1175 least because of error correction to keep the computation on track. Error correction inherently requires
1176 irreversible operations, such as supplying continuously ground-state configurations (e.g. "zero" ancilla
1177 qubits). Reversible circuits need to be adiabatic, there cannot be heat exchanges between the circuit and its
1178 environment. They must be in equilibrium at all times, which means to conserve the squared modulus of
1179 the wavefunction, and "all times" actually means during the coherence time.

1180 Two universal reversible logic gates, both operating on three bits or qubits, have been suggested to
1181 implement logically-reversible operations. The Toffoli gate (Toffoli (1982)) inverts the state of a target bit
1182 conditioned on the state of two control bits; the Fredkin gate (Fredkin and Toffoli (1982)) swaps the last
1183 two bits conditioned on the state of the control bit. In these two gates, any set of inputs is processed and
1184 results as a unique pattern of outputs; these gates are therefore logically reversible. Examples of logically
1185 reversible circuits have actually been designed and fabricated (Shao et al. (2007); Patel et al. (2016); Li et al.
1186 (2022); Orbach et al. (2012)), however they always practically display some degrees of energy dissipation
1187 by different means (e.g., requiring ancilla qubits (Ikonen et al. (2017)), finite-rate operation and read-out
1188 (Orbach et al. (2012)), and so on).

1189 Secondly, and most important, this much excitation energy to prepare the initial state, even if in principle
1190 recyclable, has to be fully available at least to start the calculation. If we assume as a practical upper
1191 bound $\epsilon_Q \simeq 10^{-5}$ and a GHz quantum computer, the minimum (reversible) E per elementary logical
1192 operation is then ~ 0.007 eV, compared to the thermal energy $\sim 10^{-6}$ eV at 30 mK. As a worst-case
1193 example (Gea-Banacloche (2002a)), let us suppose that 5000 logical qubits are needed to factor a 1000-bit
1194 number; a 7-qubit code concatenated only once (depth=2) is used for error correction; only local gates are
1195 available; and about 10 ancilla qubits per logical qubit are used. Figure 7 shows estimates of the minimum
1196 power as a function of coherence time, for a driving microwave field at frequency $\omega = (\epsilon_Q^{3/2} \tau)^{-1}$, the full
1197 and dashed lines corresponding to periodic and static excitation fields.

1198 Despite the purely heuristic nature of Eq.(73) (for example, the error limit could be improved by smarter
1199 correction algorithms, or by improved hardware solutions) the results clearly indicate that, for very large-
1200 scale quantum computations, one really needs to use quantum systems with very long decoherence times.
1201 Values of τ in the 100- μ s range would require megawatt start-up power. It is just not feasible to get around
1202 the problem of short decoherence times just by driving the system at faster frequencies. This also suggests
1203 that there could probably never be the equivalent of a "Moore's law" for quantum computers.

1204 **The required energy budget that would be needed for large-scale quantum applications has only sparsely**
1205 **been considered, up to now. Efficiency, or quantum advantage, or quantum supremacy are most often**
1206 **estimated in terms of the amount of resources needed for a quantum vs. classical computation (number of**
1207 **qubits, connections, scaling of the operations). But the final bill from the electric company will eventually**
1208 **count the watt-hours consumed, and the notion of "green quantum advantage" provides the more useful**
1209 **comparison, by looking at the amount of elementary operations performed per watt consumed (Bedingham**
1210 **and Maroney (2016); Jaschke and Montangero (2023)). A key quantity to consider is the amount of**
1211 **energy needed to implement a quantum gate in a set amount of time (Cimini et al. (2020); Deffner (2021);**
1212 **Stevens et al. (2022); Fellous-Asiani et al. (2023)). While the main concern of fundamental quantum**
1213 **computing is focused at the issues of noise reduction and protecting quantum resources from decoherence,**
1214 **the management of resources at the full-stack, macroscopic level must take into account all the enabling**
1215 **technologies that surround the quantum machine, and that make it possible to interact with and extract**
1216 **information from it. Quantum thermodynamics is but one brick of the construction that will lead to the**
1217 **future quantum computers; however, as it can be demonstrated by comparing with the historical trajectory**

1218 of classical CMOS computers, the issues around energy consumption of quantum computing represent
 1219 a crucial step, and must be faced even well before any practical machine will be operational (Auffèves
 1220 (2022); Carlesso and Paternostro (2023)).

1221 **Objectivity of measurement and "Quantum Darwinism"** In the standard circuit (or QED) model, the
 1222 array of qubits is initialized for example in the logical $|0\rangle$ state; then, a sequence of quantum gates is
 1223 applied depending on the required algorithm; finally, a read-out operation is carried out by measuring
 1224 individual qubits in the same $|0/1\rangle$ computational basis. In alternative, the adiabatic quantum computation
 1225 does not rely on gate sequences, but on the direct implementation of a smoothly varying Hamiltonian on the
 1226 network of qubits; after the initial prepared state, annealing and read-out are cyclically performed to obtain
 1227 the global optimum configuration of spins, which gives the ground state of the "solution" Hamiltonian. In
 1228 either instance, the read-out operations give a human-readable, classical physics result from the quantum
 1229 computation.

1230 The final state of the computation is something like $|\psi\rangle = \sum_n c_n |n\rangle$ and, as we know, the complex
 1231 amplitudes c_n are not directly accessible. The measurement gives one of the $n \in N$ possible outcomes
 1232 with probability $|c_n|^2$, that is a probabilistic rule for projecting the state vector onto one of the vectors of
 1233 the orthonormal measurement basis. Consider for example the general qubit state $|\psi\rangle = c_1 |0\rangle + c_2 |1\rangle$,
 1234 and assume that we want to perform a measurement in the orthonormal basis $|u\rangle = a |0\rangle + b |1\rangle$, $|v\rangle =$
 1235 $b^* |0\rangle - a^* |1\rangle$. The probability of a measurement giving $|u\rangle$ as a result is:

$$P(u) = |\langle u, \psi \rangle|^2 = |(a^* \langle 0| + b^* \langle 1|)(c_1 |0\rangle + c_2 |1\rangle)|^2 = |a^* c_1 + b^* c_2|^2 \quad (74)$$

1236 and similarly, the probability of getting $|v\rangle$:

$$P(v) = |\langle v, \psi \rangle|^2 = |(b \langle 0| - a \langle 1|)(c_1 |0\rangle + c_2 |1\rangle)|^2 = |bc_1 - ac_2|^2 \quad (75)$$

1237 Decoherence of the qubits is the loss of their typical quantum properties, entanglement and non-locality,
 1238 through interactions with the environment. New correlations with the thermal bath degrees of freedom
 1239 appear, which degrade the information originally encoded in the quantum system.

1240 In classical physics, what you see is simply "how things are". You can measure a tennis ball traveling
 1241 at 120 km/h to a given direction, passing through a given point in space at a given instant of time. What
 1242 more is there to say? But when a quantum particle is in a state of "superposition" before the measurement,
 1243 the various superposed states interfere with one another in a wavelike manner. Only when we make a
 1244 measurement we see one of those outcomes. But, given the probabilistic nature of the result, why just *that*
 1245 *one*? Could someone else check our result and find that same outcome?

1246 The definite properties that we associate with classical physics, such as position and velocity, may be
 1247 selected from a "menu" of quantum possibilities, in a process loosely analogous to natural selection in
 1248 evolution. The quantum properties that survive are - in a kind of pseudo-Darwinist sense - the "fittest" (Zurek
 1249 (1982, 2003)). And, as it happens in natural selection, the "survivors" are those that make the most copies
 1250 of themselves. Many independent observers can thus make measurements of the quantum system, each one
 1251 using a different copy of the result, and agree on the outcome - a hallmark of classical behavior. "Quantum
 1252 Darwinism" (QD, Zwolak et al. (2009); Milazzo et al. (2019); Chen et al. (2019); Ryan et al. (2021))

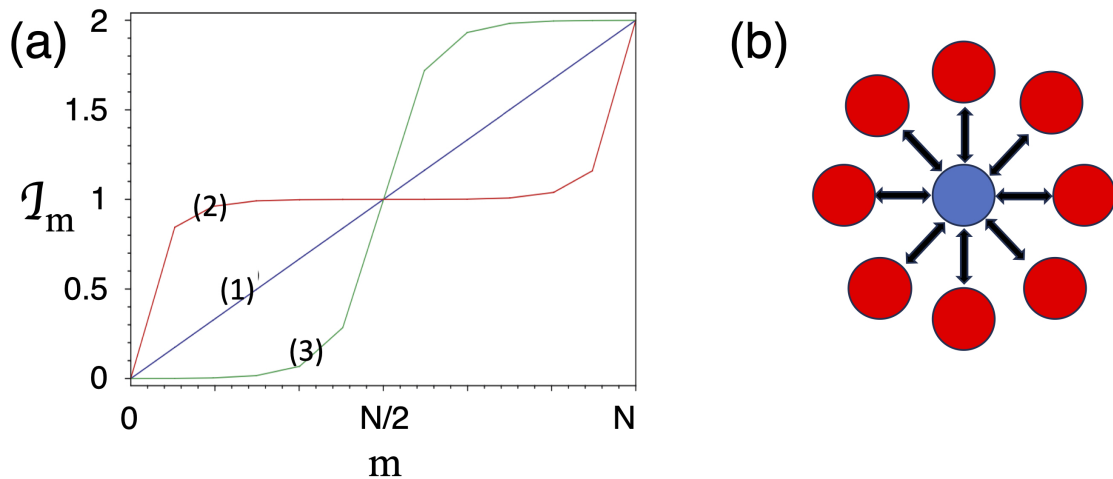


Figure 8. (a) Typical behavior of the information plots \mathcal{I}_m as a function of the fractions of environment interrogated by different observers. (b) The spin star environment.

1253 changes the role of the environment, from being a shady background with undetermined characteristics, into
 1254 a fragmented space filled with redundant information that can be accessed and "measured" by individual
 1255 observers. Notably, this notion is different from the macroscopic limit, because of which the number
 1256 of degrees of freedom of the environment is so large that the *averaging* process dominates the read-out
 1257 process; QD instead deals with the mechanism by which the quantum information gets encoded (i.e.,
 1258 entangled) to the surrounding quantum states of the environment.

1259 Experimental measurements of the result of a quantum computation are typically recorded by collecting
 1260 information transmitted through some carriers - photons, electrons, phonons - that constitute the
 1261 environment (thermal bath). While there will be many such individual information carriers, only a small
 1262 fraction typically needs to be captured in order for the observer to accurately record the measurement.
 1263 Given two observers, they will agree on the outcome when they can independently intercept different
 1264 fractions of these information carriers, and both perform the same type of measurement on their respective
 1265 sets. In the QD scheme, they will necessarily arrive at the same conclusion, due to the entanglement shared
 1266 between the system and all the environmental degrees of freedom. Then, a key question is whether is it
 1267 possible to get enough information, by monitoring only a small part of the environment?

1268 We may look at the amount of (Shannon) entropy that is produced by destroying the correlations between
 1269 the system S and a fraction $m \in N$ of the total environment E , that is the quantum mutual information \mathcal{I}
 1270 defined in Eq.(60) above, and ask how the partial information gathered compares to the whole (Blume-
 1271 Kohout and Zurek (2005)). From the obvious condition that \mathcal{I}_m must be non-decreasing, three possible
 1272 behaviors can be envisaged as shown in Figure 8a: the linear one, $\mathcal{I}_m \propto m$, in which each fraction of the
 1273 environment provides unique and independent information, so that each observer would obtain a separate
 1274 information about the system: alternatively the curve 2, describing redundantly stored information, \mathcal{I}_m
 1275 rapidly increases, then plateaus at the value for which all observers essentially obtain the same information
 1276 (the so-called "objectivity plateau"); or the curve 3, describing information about the system that is
 1277 tightly encoded, so that \mathcal{I}_m remains close to zero, then suddenly increases to the maximum around some
 1278 characteristic amount, for example $m \sim N/2$.

1279 Let us consider a quantum system S of a single qubit initially in a pure state, superposition of two states
 1280 $|\psi_1\rangle, |\psi_2\rangle$ expressed in the conventional basis $|0\rangle, |1\rangle$ (for the sake of simplicity, I avoid here the customary
 1281 introduction of the "pointer" states):

$$|\psi_S\rangle = a |\psi_1\rangle + b |\psi_2\rangle, \quad |a|^2 + |b|^2 = 1 \quad (76)$$

1282 and embedded in an "environment" of N other qubits, all in a same generic state $|\psi_E\rangle$, also expressed
 1283 in the same basis $|0\rangle, |1\rangle$ but with random coefficients. The overall initial state is assumed to be without
 1284 correlation between S and E , i.e. factorizable as :

$$|\psi_{SE}^0\rangle = (a |\psi_1\rangle + b |\psi_2\rangle) \otimes |\psi_E\rangle \quad (77)$$

1285 QD posits that, after some thermalization time, in which the coupled $S - E$ system evolves, the total
 1286 state of the system can be turned to:

$$|\psi_{SE}^t\rangle = a |1\rangle |1^{\otimes N}\rangle + b |0\rangle |0^{\otimes N}\rangle \quad (78)$$

1287 the notation $M^{\otimes N} = M \otimes M \dots \otimes M$ indicates the direct product of all environment degrees being in either
 1288 one or the other state of the computational basis.

1289 Several authors have considered the configuration as a "spin star" (e.g., Giorgi et al. (2015); Ryan et al.
 1290 (2021), see Fig.8b), in which the single qubit is a spin surrounded by a circle of environmental spins.
 1291 Different subgroups of environment spins can be read-out by different observers, without perturbing the
 1292 central spin, which interacts independently and equally with each one of the subsystems

1293 If now we take the partial trace over the N qubits (spins) of the environment, the density matrix for S is
 1294 obtained:

$$\rho_S = |a|^2 |\psi_1\rangle \langle \psi_1| + |b|^2 |\psi_2\rangle \langle \psi_2| \quad (79)$$

1295 while each of the environment qubits has the same density matrix:

$$\rho_{E_i} = |a|^2 |0\rangle \langle 0| + |b|^2 |1\rangle \langle 1| \quad (80)$$

1296 The crucial point is that, although the system S has lost its coherence, the population coefficients (a, b) of
 1297 the qubit S are "imprinted" on each of the N environment qubits, generating a redundancy of information.
 1298 This is the phenomenon manifested in the "plateau" of constant information seen in Fig.8a, curve (2).
 1299 Then, different observers measuring only a subset of the final state will agree on the result. And this should
 1300 represent the emergence of classical objectivity.

7 CONCLUSIONS

1301 This overview tried to provide a (necessarily limited and incomplete) synthesis of some outstanding issues
1302 in the definition of thermodynamic concepts at the level of quantum mechanics, under the peculiar angle of
1303 their possible and likely impact on quantum computer technology, and quantum computing algorithms. This
1304 field has known a rapid growth in the past decades, moving from the domain of theoretical speculations,
1305 to the urgent requirement of starting to provide real solutions to practical problems that the quantum
1306 computing hardware is facing. Despite the main technical difficulties today still lie in the probabilistic
1307 nature of the quantum computing output and the need for error correction, it is possible that thermal limits
1308 will represent the next hurdle for the efficient and useful operation of such machines.

1309 It may look surprising that the historical and philosophical discussions about the Second Law of
1310 thermodynamics should have an interest, and even represent a foundation for practical quantum computing.
1311 The relationship between information theory, manipulation of information at small scales (which also
1312 interests other fields, such as molecular and DNA-based computing, see e.g. Kempes et al. (2017); Daley
1313 and Kari (2002)) and thermodynamics is not purely formal, but treats information as a physical entity. The
1314 contribution of fluctuation theorems and stochastic thermodynamics provides a more ample framework for
1315 analyzing quantum information and exchanges of work and heat in open quantum systems. The definition
1316 of quantum entropy (Von Neumann's, despite some ambiguities, or other competing definitions) is also key
1317 in the attempt at understanding the emergence of macroscopic information in the measurement process.

1318 Still, several problems and questions remain open, both at the fundamental- and applied-physics level.
1319 For example, the definition of quantum equivalents of work and heat given in Eq.(50) and the path-integral
1320 form in Eq.(52) refer to different situations. While the latter, fluctuation-based concept is applicable in
1321 general to either closed or open systems, the "weak" form refers to the average energy exchanges (ensemble
1322 averages) in and out of the system. In most cases these (and a couple other) different definitions arrive in
1323 practice at the same results, however our understanding of the question still appears not solid enough, and
1324 open to further investigation.

1325 At first, entanglement seems to be unrelated to thermodynamics. However, the challenge of maintaining
1326 entangled states is linked to the interaction of qubits with the environment, that is a thermal bath.
1327 Quantum decoherence, or the loss of off-diagonal components in the density matrix, is the process
1328 that eventually undermines entanglement, by transfer of entangled states between the computing qubits and
1329 the environment's quantum states. There is a whole thermodynamic domain that I did not touch in this
1330 article, that is quantum batteries (Bhattacharjee and Dutta (2021); Shi et al. (2022)), whose key problem is
1331 to quantify the maximum extractable work, and which crucially depends on the interplay of coherence and
1332 entanglement between the quantum battery and the charger.

1333 Quantum computers can check and verify the theoretical predictions of quantum thermodynamics, and
1334 quantum thermodynamics will, in turn, help to quantify and master dissipative processes in quantum
1335 computing. The interplay of quantum mechanics and thermodynamics is a young research field, still rich of
1336 interesting issues and open questions.

CONFLICT OF INTEREST STATEMENT

1337 The author declares no competing interests.

AUTHOR CONTRIBUTIONS

1338 FC assembled all the materials and compiled the original manuscript.

FUNDING

1339 Institutional funding from IEMN CNRS and the University of Lille is acknowledged.

ACKNOWLEDGMENTS

1340 I gratefully thank my colleagues Valérie Vallet and Stephan De Bievre for their kind invitation to the
1341 Quantum Information Working Group, in the University of Lille, which provided the excuse to assemble
1342 these lectures. Several useful discussions with Stefano Giordano (IEMN) are also gratefully acknowledged.

DATA AVAILABILITY STATEMENT

1343 All data that is used is public and referred to by references, footnotes or otherwise in the article.

REFERENCES

- 1344 Aaronson, S. and Arkhipov, A. (2011). The computational complexity of linear optics. In *STOC '11: Proceedings of the forty-third annual ACM symposium on theory of computing*, eds. L. Fortnow and
1345 S. Vadhan (New York, NY: ACM), 333–342
- 1347 Aghaee, M., Akkala, A., Alam, Z., Ali, R., Ramirez, A. A., Andrzejczuk, M., et al. (2023). InAs-Al hybrid
1348 devices passing the topological gap protocol. *Phys. Rev. B* 107, 245423
- 1349 Agrawal, M., Kayal, N., and Saxena, N. (2004). Primes in p. *Ann. Math.* 160, 781–793
- 1350 Alemany, A. and Ritort, F. (2010). Fluctuation theorems in small systems: extending thermodynamics to
1351 the nanoscale. *Europhys. News* 41, 27–30
- 1352 Amico, M., Saleem, Z. H., and Kumph, M. (2019). An experimental study of Shor's factoring algorithm
1353 on IBM Q. *Phys. Rev. A* 100, 012305
- 1354 Anaya-Contreras, J. A., Moya-Cessa, H. M., and Zúniga-Segundo, A. (2019). The Von Neumann entropy
1355 for mixed states. *Entropy* 21, 49
- 1356 Araki, H. and Lieb, E. H. (1970). Entropy inequalities. *Commun. Math. Phys.* 18, 160–170
- 1357 Arute, F., Arya, K., Babbush, R., Bacon, D., Bardin, J. C., Barends, R., et al. (2019). Quantum supremacy
1358 using a programmable superconducting processor. *Nature* 574, 505–510
- 1359 Auffèves, A. (2022). Quantum technologies need a quantum energy initiative. *PRX Quantum* 3, 020101
- 1360 Bedingham, D. J. and Maroney, O. J. E. (2016). The thermodynamic cost of quantum operations. *New J.*
1361 *Phys.* 18, 113050
- 1362 Bender, C. M., Brody, D. C., and Meister, B. K. (2000). Quantum mechanical Carnot engine. *J. Phys. A:*
1363 *Math. Gen.* 33, 4427
- 1364 Benenti, G., Casati, G., Saito, K., and Whitney, R. S. (2017). Fundamental aspects of steady-state
1365 conversion of heat to work at the nanoscale. *Phys. Rep.* 694, 1–124
- 1366 Bennett, C. H. (1982). The thermodynamics of computation - a review. *Int. J. Theor. Phys.* 21, 905–940
- 1367 Bennett, C. H., DiVincenzo, D. P., Smolin, J. A., and Wootters, W. K. (1996). Mixed-state entanglement
1368 and quantum error correction. *Phys. Rev. A* 54, 3824
- 1369 Bennett, C. H., Grudka, A., Horodecki, M., Horodecki, P., and Horodecki, R. (2011). Postulates for
1370 measures of genuine multipartite correlations. *Phys. Rev. A* 83, 012312

- 1371 Bernstein, E. and Vazirani, U. V. (1997). Quantum complexity theory. *SIAM J. Comput.* 26, 1411–1473
- 1372 Bèrut, A., Arakelyan, A., Petrosyan, A., Ciliberto, S., Dillenschneider, R., and Lutz, E. (2011).
1373 Experimental verification of Landauer’s principle linking information and thermodynamics. *Nature* 483,
1374 187–189
- 1375 Bespalov, V. A., Dyuzhev, N. A., and Kireev, V. Y. (2022). Possibilities and limitations of CMOS
1376 technology for the production of various microelectronic systems and devices. *Nanobiotech. Rep.* 17,
1377 24–38
- 1378 Bhattacharjee, S. and Dutta, A. (2021). Quantum thermal machines and batteries. *Eur. Phys. J. B* 94, 239
- 1379 Blais, A., Grimsmo, A. L., Girvin, S. M., and Walraff, A. (2021). Circuit quantum electrodynamics. *Rev.*
1380 *Mod. Phys.* 93, 025005
- 1381 Blume-Kohout, R. and Zurek, W. H. (2005). A simple example of ”Quantum Darwinism”: Redundant
1382 information storage in many-spin environments. *Found. Phys.* 35, 1857–1876
- 1383 Boudot, F., Gaudry, P., Guillevic, A., Heninger, N., Thomé, E., and Zimmermann, P. (2020). Comparing
1384 the difficulty of factorization and discrete logarithm: a 240-digit experiment. In *The 40th Annual*
1385 *International Cryptology Conference (Crypto 2020)* (Santa Barbara, California, USA: IACR)
- 1386 Breitenbach, G., Schiller, S., and Mlynek, J. (1997). Measurement of the quantum states of squeezed light.
1387 *Nature* 387, 471–475
- 1388 Breuer, H.-P., Laine, E.-M., Piilo, J., and Vacchini, B. (2016). Non-Markovian dynamics in open quantum
1389 systems. *Rev. Mod. Phys.* 88, 021002
- 1390 Breuer, H. P. and Petruccione, F. (2002). *The theory of open quantum systems*. (Oxford, UK: Clarendon
1391 Press)
- 1392 Brooks, P., Kitaev, A., and Preskill, J. (2013). Protected gates for superconducting qubits. *Phys. Rev. A* 87,
1393 052306
- 1394 Bruzewicz, C. D., Chiaverini, J., McConnell, R., and Sage, J. M. (2019). Trapped-ion quantum computing:
1395 Progress and challenges. *Appl. Phys. Rev.* 6, 021413
- 1396 Brydges, T., Elben, A., Jurcevic, P., Vermersch, B., Maier, C., Lanyon, B. P., et al. (2019). Probing Rényi
1397 entanglement entropy via randomized measurements. *Science* 364, 260
- 1398 Caban, P., Rembieliński, J., Smoliński, K. A., and Walczak, Z. (2015). Classification of two-qubit states.
1399 *Quantum Inf. Proc.* 14, 4665–4690
- 1400 Carlesso, M. and Paternostro, M. (2023). From basic science to technological development: The case for
1401 two avenues. In *Photonic Quantum Technologies: Science and Applications.*, ed. M. Beyounef (New
1402 York: J. Wiley). ch.6
- 1403 Chen, M.-C., Zhong, H.-S., Li, Y., Wu, D., Wang, X.-L., Li, L., et al. (2019). Emergence of classical
1404 objectivity on a quantum Darwinism simulator. *Sci. Bull.* 64, 580
- 1405 Cheng, B., Deng, X.-H., Gu, X., He, Y., Hu, G., Huang, P., et al. (2023). Noisy intermediate-scale quantum
1406 computers. *Front. Phys.* 18, 21308
- 1407 Cherian, J. P., Chakraborty, S., and Ghosh, S. (2019). On thermalization of two-level quantum systems.
1408 *Europhys. Lett.* 126, 40003
- 1409 Cimini, V., Gherardini, S., Barbieri, M., Gianani, I., Sbroscia, M., Buffoni, L., et al. (2020). Experimental
1410 characterization of the energetics of quantum logic gates. *npj Quantum Inf.* 6, 96
- 1411 Collin, D., Ritort, F., Jarzynski, C., Smith, S. B., Tinoco, I., and Bustamante, C. (2005). Verification of the
1412 Crooks fluctuation theorem and recovery of RNA folding free energies. *Nature* 437, 231–234
- 1413 Crooks, G. (1999). Entropy production fluctuation theorem and the nonequilibrium work relation for free
1414 energy differences. *Phys. Rev. E* 60, 2721

- 1415 da Silva, M. P., Ryan-Anderson, C., Bello-Rivas, J. M., Chernoguzov, A., Dreiling, J. M., Foltz, C., et al.
1416 (2024). Demonstration of logical qubits and repeated error correction with better-than-physical error
1417 rates. Preprint at <https://doi.org/10.48550/arXiv.2404.02280>
- 1418 Daley, M. J. and Kari, L. (2002). DNA computing: models and implementations. *Comm. Theor. Biol.* 7,
1419 177–198
- 1420 Dann, R., Kosloff, R., and Salamon, P. (2020). Quantum finite-time thermodynamics: Insight from a single
1421 qubit engine. *Entropy* 22, 1255
- 1422 Deffner, S. (2021). Energetic cost of Hamiltonian quantum gates. *Europhys. Lett.* 134, 40002
- 1423 Editorial (2022). (special issue) 40 years of quantum computing. *Nature Rev. Phys.* 4, 1
- 1424 Einstein, A. (1916). Strahlungs-Emission und -Absorption nach der Quantentheorie. In *The collected*
1425 *papers of Albert Einstein. Vol. 6. The Berlin years.*, eds. A. J. Kox, M. J. Klein, and R. Schulmann ((engl.
1426 transl.): Princeton Univ. Press). 364
- 1427 Esteve, J., Gross, C., Weller, A., Giovanazzi, S., and Oberthaler, M. (2008). Squeezing and entanglement
1428 in a Bose-Einstein condensate. *Nature* 455, 1216–1219
- 1429 Evans, D. J., Cohen, E. G., and Morriss, G. P. (1993). Probability of second law violations in shearing
1430 steady states. *Phys. Rev. Lett.* 71, 2401–2404
- 1431 Fellous-Asiani, M., Chai, J. H., Thonnart, Y., Ng, H. K., Whitney, R. S., and Auffèves, A. (2023).
1432 Optimizing resource efficiencies for scalable full-stack quantum computers. *PRX Quantum* 4, 040319
- 1433 Feynman, R. P. (1982). Simulating physics with computers. *Int. J. Theor. Phys.* 21, 467–488
- 1434 Feynman, R. P. (1985). Quantum mechanical computers. *Opt. News* 11, 11
- 1435 Figgatt, C., Ostrander, A., Linke, N. M., Landsman, K. A., Zhu, D., Maslov, D., et al. (2019). Parallel
1436 entangling operations on a universal ion-trap quantum computer. *Nature* 572, 368–372
- 1437 Fitzpatrick, M., Sundaresan, N. M., Li, A. C. Y., Koch, J., and Houck, A. A. (2017). Observation of a
1438 dissipative phase transition in a one-dimensional circuit QED lattice. *Phys. Rev. X* 7, 011016
- 1439 Franco, R. L. and Compagno, G. (2016). Quantum entanglement of identical particles by standard
1440 information-theoretic notions. *Sci. Rep.* 6, 20603
- 1441 Fredkin, E. and Toffoli, T. (1982). Conservative logic. *Int. J. Theor. Phys.* 21, 219–253
- 1442 Frey, M. R. (2016). Quantum speed limits - Primer, perspectives, and potential future directions,. *Quant.*
1443 *Inf. Proc.* 15, 3919
- 1444 Friis, N., Vitagliano, G., Malik, M., and Huber, M. (2019). Entanglement certification from theory to
1445 experiment. *Nature Rev. Phys.* 1, 72
- 1446 García-Saez, A., Ferraro, A., and Acín, A. (2009). Local temperature in quantum thermal states. *Phys. Rev.*
1447 *A* 79, 052340
- 1448 Gea-Banacloche, J. (2002a). Minimum energy requirements for quantum computation. *Phys. Rev. Lett.* 89,
1449 217901
- 1450 Gea-Banacloche, J. (2002b). Some implications of the quantum nature of laser fields for quantum
1451 computations. *Phys. Rev. A* 65, 022308
- 1452 Geusic, J. E., Schulz-DuBois, E. O., and Scovil, H. K. D. (1967). Quantum equivalent of the Carnot cycle.
1453 *Phys. Rev.* 156, 343–351
- 1454 Geva, E. and Kosloff, R. (1992). A quantum-mechanical heat engine operating in finite time. A model
1455 consisting of spin-1/2 systems as the working fluid. *J. Chem. Phys.* 96, 3054–3067
- 1456 Ghonge, S. and Vural, D. C. (2018). Temperature as a quantum observable. *J. Stat. Mech. Theor. Expt.*
1457 2018, 073102
- 1458 Gil, D. and Green, W. M. J. (2020). The future of computing: bits + neurons + qubits. In *International*
1459 *Solid-State Circuits Conference ISSCC-30* (New York: IEEE), 30–39

- 1460 Giordani, T., Hoch, F., Carvacho, G., Spagnolo, N., and Sciarrino, F. (2023). Integrated photonics in
1461 quantum technologies. *Riv. Nuovo Cim.* 46, 71–103
- 1462 Giorgi, G. L., Galve, F., and Zambrini, R. (2015). Quantum Darwinism and non-Markovian dissipative
1463 dynamics from quantum phases of the spin1/2 XX model. *Phys. Rev. A* 92, 022105
- 1464 Girolami, D., Tufarelli, T., and Susa, C. E. (2017). Quantifying genuine multipartite correlations and their
1465 pattern complexity. *Phys. Rev. Lett.* 119, 140505
- 1466 Goldstein, S., Lebowitz, J. L., Tumulka, R., and Zanghì, N. (2020). Gibbs and Boltzmann entropy in
1467 classical and quantum mechanics. In *Statistical mechanics and scientific explanation*, ed. V. Allori
1468 (Singapore: World Scientific). 519–581
- 1469 Goold, J., Huber, M., Riera, A., del Rio, L., and Skrzypczyk, P. (2016). The role of quantum information
1470 in thermodynamics - a topical review. *J. Phys. A* 49, 143001
- 1471 Guhne, O. and Toth, G. (2009). Entanglement detection. *Phys. Rep.* 474, 1
- 1472 Gyenis, A., Mundada, P. S., Paolo, A. D., Hazard, T. M., You, X., Schuster, D. I., et al. (2021). Experimental
1473 realization of an intrinsically error-protected superconducting qubit. *PRX Quantum* 2, 010339
- 1474 Hänggi, M. C. P. and Talkner, P. (2011). Quantum fluctuation relations: Foundations and applications. *Rev.*
1475 *Mod. Phys.* 83, 771
- 1476 Hanson, R., Dobrovitski, V. V., Feiguin, A. E., Gywat, O., and Awschalom, D. D. (2008). Coherent
1477 dynamics of a single spin interacting with an adjustable spin bath,. *Science* 352, 633
- 1478 Hanson, R., van Beveren, L. H. W., Vink, I. T., Elzerman, J. M., Naber, W. J. M., Koppens, F. H. L., et al.
1479 (2005). Single-shot readout of electron spin states in a quantum dot using spin-dependent tunnel rates.
1480 *Phys. Rev. Lett.* 94, 196802
- 1481 Harris, R., Sato, Y., Berkley, A. J., Reis, M., Altomare, F., Amin, M. H., et al. (2018). Phase transitions in
1482 a programmable quantum spin glass simulator. *Science* 361, 162–165
- 1483 Hartmann, M. and Mahler, G. (2005). Measurable consequences of the local breakdown of the concept of
1484 temperature. *Europhys. Lett.* 70, 579
- 1485 Hauke, P., Katzgraber, H. G., Lechner, W., Nishimori, H., and Oliver, W. D. (2020). Perspectives of
1486 quantum annealing: methods and implementations. *Rep. Prog. Phys.* 83, 054401
- 1487 Henao, I. and Serra, R. M. (2018). Role of quantum coherence in the thermodynamics of energy transfer.
1488 *Phys. Rev. E* 97, 062105
- 1489 Hill, S. A. and Wootters, W. K. (1997). Entanglement of a pair of quantum bits. *Phys. Rev. Lett.* 78, 5022
- 1490 Hime, T., Reichardt, P. A., Plourde, B. L. T., Robertson, T. L., Wu, C.-E., Ustinov, A. V., et al. (2006).
1491 Solid-state qubits with current-controlled coupling. *Science* 314, 1427–1429
- 1492 Huang, H.-L., Wu, D., Fan, D., and Zhu, X. (2020). Superconducting quantum computing: a review.
1493 *Science China* 63, 180501
- 1494 Huang, X. L., Xu, H., Niu, X. Y., and Fu, Y. D. (2013). A special entangled quantum heat engine based on
1495 the two-qubit Heisenberg XX model. *Phys. Scr.* 88, 065008
- 1496 Huber, M., Perarnau-Llobet, M., Hovhannisyan, K. V., Skrzypczyk, P., Klöckl, C., Brunner, N., et al.
1497 (2015). Thermodynamic cost of creating correlations. *New J. Phys.* 17, 065008
- 1498 Ikonen, J., Salmilehto, J., and Möttönen, M. (2017). Energy-efficient quantum computing. *npj Quant. Inf.*
1499 3, 17
- 1500 Jäger, S. B., Schmit, T., Morigi, G., Holland, M. J., and Betzholz, R. (2022). Lindblad master equations for
1501 quantum systems coupled to dissipative bosonic modes. *Phys. Rev. Lett.* 129, 063601
- 1502 Jarzynski, C. (1997). Nonequilibrium equality for free energy differences. *Phys. Rev. Lett.* 78, 2690–2693
- 1503 Jaschke, D. and Montangero, S. (2023). Is quantum computing green? an estimate for an energy-efficiency
1504 quantum advantage. *Quantum Sci. Techn* 8, 025001

- 1505 Jaynes, E. T. (1965). Gibbs vs Boltzmann entropies. *Am. J. Phys.* 33, 391–398
- 1506 Johnson, J. B. (1928). Thermal agitation of electricity in conductors. *Phys. Rev.* 32, 97–109
- 1507 Kempes, C. P., Wolpert, D., Cohen, Z., and Pérez-Mercader, J. (2017). The thermodynamic efficiency of
1508 computations made in cells across the range of life. *Philos., Trans. A Math. Phys. Eng.* 375, 2016343
- 1509 Kim, Y., Eddins, A., Anand, S., Wei, K. X., van den Berg, E., Rosenblatt, S., et al. (2023a). Evidence for
1510 the utility of quantum computing before fault tolerance. *Nature* 618, 500–505
- 1511 Kim, Y., Eddins, A., Anand, S., Wei, K. X., van den Berg, E., Rosenblatt, S., et al. (2023b). Evidence for
1512 the utility of quantum computing before fault tolerance. *Nature* 618, 500–505
- 1513 Kish, L. B. (2002). End of Moore’s law: thermal (noise) death of integration in micro and nano electronics.
1514 *Phys. Lett. A* 305, 144–149
- 1515 Kjaergaard, M., Schwartz, M. E., Braumüller, J., Krantz, P., Wang, J. I.-J., Gustavsson, S., et al. (2020).
1516 Superconducting qubits: Current state of play. *Ann. Rev. Cond. Matt. Phys.* 11, 369–395
- 1517 Knill, E., Laflamme, R., and Milburn, G. J. (2001). A scheme for efficient quantum computation with
1518 linear optics. *Nature* 409, 46–52
- 1519 Koch, J., Yu, T. M., Gambetta, J., Houck, A. A., Schuster, D. I., Majer, J., et al. (2007). Charge-insensitive
1520 qubit design derived from the Cooper pair box. *Phys. Rev. A* 76, 042319
- 1521 Kohler, S. (2017). Dispersive readout of adiabatic phases. *Phys. Rev. Lett.* 119, 196802
- 1522 Kohler, S. (2018). Dispersive readout: Universal theory beyond the rotating-wave approximation. *Phys.*
1523 *Rev. A* 98, 023849
- 1524 Koski, J., Maisi, V., Sagawa, T., and Pekola, J. P. (2014). Experimental observation of the role of mutual
1525 information in the nonequilibrium dynamics of a maxwell demon. *Phys. Rev. Lett.* 113, 030601
- 1526 Kosloff, R. (2013). Quantum thermodynamics: a dynamical viewpoint. *Entropy* 15, 2100–2128
- 1527 Kubo, Y., Ong, F. R., Bertet, P., Vion, D., Jacques, V., Zheng, D., et al. (2010). Strong coupling of a spin
1528 ensemble to a superconducting resonator. *Phys. Rev. Lett.* 105, 140502
- 1529 Ladyman, J., Presnell, S., Short, A. J., and Groisman, B. (2007). The connection between logical and
1530 thermodynamic irreversibility. *Studies Hist. Phil. Sci. B* 38, 58–79
- 1531 Landauer, R. (1961). Irreversibility and heat generation in the computing process. *IBM Journal* July,
1532 183–191
- 1533 Li, Y., Wan, L., Zhang, H., Zhu, H., Shi, Y., Chin, L. K., et al. (2022). Quantum Fredkin and Toffoli gates
1534 on a versatile programmable silicon photonic chip. *npj Quant. Inf.* 8, 112
- 1535 Liang, Y.-C., Yeh, Y.-H., Mendonca, P. E. M. F., Teh, R. Y., Reid, M. D., and Drummond, P. D. (2019).
1536 Quantum fidelity measures for mixed states. *Rep. Prog. Phys.* 82, 076001
- 1537 Lin, B. and Chen, J. (2003). Performance analysis of an irreversible quantum heat engine working with
1538 harmonic oscillators. *Phys. Rev. E* 67, 046105
- 1539 Lindblad, G. (1976). On the generators of quantum dynamical semigroups. *Commun. Math. Phys.* 48, 119
- 1540 Lipka-Bartosik, P., Perarnau-Llobet, M., and Brunner, N. (2023). Operational definition of the temperature
1541 of a quantum state. *Phys. Rev. Lett.* 130, 040401
- 1542 Liu, Y. A., Liu, X. L., Li, F. N., Fu, H., Yang, Y., Song, J., et al. (2021). Closing the “quantum supremacy”
1543 gap: achieving real-time simulation of a random quantum circuit using a new Sunway supercomputer. In
1544 *SC ’21: Proceedings of the International Conference for High Performance Computing, Networking,*
1545 *Storage and Analysis*, eds. B. R. D. Supinski, M. Hall, and T. Gamblin (New York: ACM, Association
1546 for Computing Machinery), 1–12
- 1547 Liu, Z., Zeng, P., Zhou, Y., and Gu, M. (2022). Characterizing correlation within multipartite quantum
1548 systems via local randomized measurements. *Phys. Rev. A* 105, 022407

- 1549 Lloyd, S. (1989). Use of mutual information to decrease entropy: Implications for the second law of
1550 thermodynamics. *Phys. Rev. A* 39, 5378
- 1551 Lo, C. F., Liu, K. L., Ng, K. M., and Yuen, P. H. (1998). Is there a spontaneous breaking of the
1552 parity symmetry of the Jaynes-Cummings model without the rotating-wave approximation?. *Quantum*
1553 *Semiclass. Opt.* 10, L63
- 1554 Ma, R., Saxberg, B., Owens, C., Leung, N., Yao, L., Simon, J., et al. (2019). A dissipatively stabilized
1555 Mott insulator of photons. *Nature* 566, 51–57
- 1556 Madsen, L. S., Laudenbach, F., Falamarzi, M., Askarani, Rortais, F., Vincent, T., et al. (2022). Quantum
1557 computational advantage with a programmable photonic processor. *Nature* 606, 75–81
- 1558 Majer, J., Chow, J. M., Gambetta, J. M., Koch, J., Johnson, B. R., Schreier, J. A., et al. (2007). Coupling
1559 superconducting qubits via a cavity bus. *Nature* 449, 443–447
- 1560 Mallet, F., Ong, F. R., Palacios-Laloy, A., Nguyen, F., Bertet, P., Vion, D., et al. (2009). RF-driven
1561 Josephson bifurcation amplifier for quantum measurement. *Nature Phys.* 5, 791–795
- 1562 Manucharyan, V. E., Koch, J., Glazman, L., and Devoret, M. (2009). Fluxonium: single cooper-pair circuit
1563 free of charge offsets. *Science* 326, 113–116
- 1564 Manzano, D. (2020). A short introduction to the Lindblad master equation. *AIP Adv.* 10, 025106
- 1565 Marcos, D., Wubs, M., Taylor, J. M., Aguado, R., Lukin, M. D., and Sørensen, A. S. (2010). Entanglement
1566 of a pair of quantum bits. *Phys. Rev. Lett.* 105, 210501
- 1567 Marcus, M. and Minc, H. (1965). Permanents. *Amer. Math. Monthly* 72, 577–591
- 1568 Martinis, J. M., Nam, S., Aumentado, J., and Urbina, C. (2002). Rabi oscillations in a large Josephson-
1569 junction qubit. *Phys. Rev. Lett.* 89, 117901
- 1570 Martín-López, E., and Thomas Lawson, A. L., Alvarez, R., Zhou, X.-Q., and O'Brien, J. L. (2012).
1571 Experimental realization of Shor's quantum factoring algorithm using qubit recycling. *Nature Phot.* 6,
1572 773–776
- 1573 Maslov, D., Dueck, G. W., Miller, D. M., and Negrevergne, C. (2008). Quantum circuit simplification and
1574 level compaction. *IEEE Trans. Comput.-Aided Design Integr. Circuits Syst.* 27, 436–444
- 1575 Micadei, K., Peterson, J. P. S., Souza, A. M., Sarthour, R. S., Oliveira, I. S., Landi, G. T., et al. (2019).
1576 Reversing the direction of heat flow using quantum correlations. *Nature Comm.* 10, 2456
- 1577 Milazzo, N., Lorenzo, S., Paternostro, M., and Palma, G. M. (2019). Role of information backflow in the
1578 emergence of quantum Darwinism. *Phys. Lett. A* 100, 012101
- 1579 Moll, N., Barkoutsos, P., Bishop, L. S., Chow, J. M., Cross, A., Egger, D. J., et al. (2018). Quantum
1580 optimization using variational algorithms on near-term quantum devices. *Quantum Sci. Tech.* 3, 030503
- 1581 Moskalenko, I. N., Simakov, I. A., Abramov, N. N., Grigorev, A. A., Moskalev, D. O., Pishchimova, A. A.,
1582 et al. (2022). High fidelity two-qubit gates on fluxonium using a tunable coupler. *npj Quantum Inf.* 8,
1583 130
- 1584 Nyquist, H. (1928). Thermal agitation of electric charge in conductors. *Phys. Rev.* 32, 110–113
- 1585 Oliver, W. and Welander, P. (2013). Materials in superconducting quantum bits. *MRS Bull.* 38, 816
- 1586 Onsager, L. (1949). Statistical hydrodynamics. *Nuovo Cim.* 6, 279–287
- 1587 Orbach, R., Remacle, F., Levine, R. D., and Willner, I. (2012). Logic reversibility and thermodynamic
1588 irreversibility demonstrated by DNAzyme-based Toffoli and Fredkin logic gates. *Proc. Nat. Ac. Sci.*
1589 109, 21228–21233
- 1590 Parrondo, J. M. R., Horowitz, J. M., and Sagawa, T. (2015). Thermodynamics of information. *Nature Phys.*
1591 11, 131–139
- 1592 Patel, R. B., Ho, J., Ferreyrol, F., Ralph, T. C., and Pryde, G. J. (2016). A quantum Fredkin gate. *Science*
1593 *Adv.* 2, e1501531

- 1594 Pelucchi, E., Fagas, G., Aharonovich, I., Englund, D., Figueroa, E., Gong, Q., et al. (2022). The potential
1595 and global outlook of integrated photonics for quantum technologies. *Nature Rev. Phys.* 4, 194–208
- 1596 Pop, I. M., Geerlings, K., Catelani, G., Schoelkopf, R. J., Glazman, L. I., and Devoret, M. H. (2014).
1597 Coherent suppression of electromagnetic dissipation due to superconducting quasiparticles. *Nature* 508,
1598 369–372
- 1599 Quan, H., Liu, Y. X., Sun, C., and Nori, F. (2007). Quantum thermodynamic cycles and quantum heat
1600 engines. *Phys. Rev. E* 76, 031105
- 1601 Rahamim, H. J., Behrle, T., Peterer, M. J., Patterson, A., Spring, P. A., Tsunoda, T., et al. (2017).
1602 Double-sided coaxial circuit QED with out-of-plane wiring. *Appl. Phys. Lett.* 110, 222602
- 1603 Ramsey, N. (1956). Thermodynamics and statistical mechanics at negative absolute temperatures. *Phys.*
1604 *Rev.* 103, 20–28
- 1605 Räsänen, M., Mäkynen, H., Mottönen, M., and Goetz, J. (2021). Path to European quantum unicorns.
1606 *EPJ Quantum Tech.* 8, 5
- 1607 Rau, J. (2009). On quantum vs. classical probability. *Annals Phys.* 324, 2622–2637
- 1608 Reeb, D. and Wolf, M. M. (2014). An improved Landauer principle with finite-size corrections. *New J.*
1609 *Phys.* 16, 103011
- 1610 Rice, S. O. (1945). Mathematical analysis of random noise. *Bell Syst. Tech. J.* 24, 46–156
- 1611 Ronnow, T. F., Wang, Z., Job, J., Boixo, S., Isakov, S. V., Wecker, D., et al. (2014). Defining and detecting
1612 quantum speedup. *Science* 345, 420–424
- 1613 Rosnagel, J., Abah, O., Schmidt-Kaler, F., and Lutz, E. (2014). Nanoscale heat engine beyond the Carnot
1614 limit. *Phys. Rev. Lett.* 112, 030602
- 1615 Rosnagel, J., Dawkins, S. T., Tolazzi, K. N., Abah, O., Lutz, E., Schmidt-Kaler, F., et al. (2016). A
1616 single-atom heat engine. *Science* 352, 325–329
- 1617 Ryan, E., Paternostro, M., and Campbell, S. (2021). Quantum Darwinism in a structured spin environment.
1618 *Phys. Lett. A* 416, 127675
- 1619 Saslow, W. M. (2020). A history of thermodynamics: The missing manual. *Entropy* 22, 77
- 1620 Schäfer, V. M., Ballance, C. J., Thirumalai, K., Stephenson, L. J., Ballance, T. G., Steane, A. M., et al.
1621 (2018). Fast quantum logic gates with trapped-ion qubits. *Nature* 555, 75
- 1622 Schymik, K.-N., Ximenez, B., Bloch, E., Dreon, D., Signoles, A., Nogrette, F., et al. (2022). In-situ
1623 equalization of single-atom loading in large-scale optical tweezer arrays. *Phys. Rev. A* 106, 022611
- 1624 Scovil, H. E. D. and Schulz-DuBois, E. O. (1959). Three-level masers as heat engines. *Phys. Rev. Lett.* 2,
1625 262
- 1626 Shannon, C. E. (1948). A mathematical theory of communication (I and II). *Bell Syst. Tech. J.* 27, 379–423,
1627 623–656
- 1628 Shao, X.-Q., Zhu, A.-D., Zhang, S., Chung, J.-S., and Yeon, K.-H. (2007). Efficient scheme
1629 for implementing an N-qubit Toffoli gate by a single resonant interaction with cavity quantum
1630 electrodynamics. *Phys. Rev. A* 75, 034307
- 1631 Shen, H. Z., Qin, M., and Yi, X. X. (2013). Single-photon storing in coupled non-Markovian atom-cavity
1632 system. *Phys. Rev. A* 88, 033835
- 1633 Shen, H. Z., Wang, Q., and Yi, X. X. (2022). Dispersive readout with non-Markovian environments. *Phys.*
1634 *Rev. A* 105, 023707
- 1635 Shi, H.-L., Ding, S., Wan, Q.-K., Wang, X.-H., and Yang, W.-L. (2022). Entanglement, coherence, and
1636 extractable work in quantum batteries. *Phys. Rev. Lett.* 129, 130602

- 1637 Shor, P. (2004). Algorithms for quantum computation: Discrete logarithms and factoring. In *Proceedings*
1638 *35th Annual Symposium on Foundations of Computer Science* (New York, NY: IEEE Comp. Soc. Press),
1639 124–134
- 1640 Shor, P. (2007). Polynomial-time algorithms for prime factorization and discrete logarithms on a quantum
1641 computer. *SIAM J. Comp.* 26, 1484–1509
- 1642 Siddiqi, I., Vijay, R., Pierre, F., Wilson, C. M., Metcalfe, M., Rigetti, C., et al. (2004). RF-driven Josephson
1643 bifurcation amplifier for quantum measurement. *Phys. Rev. Lett.* 93, 207002
- 1644 Slussarenko, S. and Pryde, G. J. (2019). Photonic quantum information processing: A concise review. *Appl.*
1645 *Phys. Rev.* 6, 041303
- 1646 Somaschi, N., Maring, N., Belabas, N., Senellart, P., Senellart, J., and Mansfield, S. (2024). A
1647 general-purpose single-photon-based quantum computing platform. In *Proc. SPIE PC12911, Quantum*
1648 *Computing, Communication, and Simulation IV* (San Francisco, USA: SPIE), PC129110M
- 1649 Steane, A. M., Imreh, G., Home, J. P., and Leibfried, D. (2014). Pulsed force sequences for fast
1650 phase-insensitive quantum gates in trapped ions. *New J. Phys.* 16, 053049
- 1651 Stehlik, J., Zajac, D. M., Underwood, D. L., Phung, T., Blair, J., Carnevale, S., et al. (2021). Tunable
1652 coupling architecture for fixed-frequency transmon superconducting qubits. *Phys. Rev. Lett.* 127, 080505
- 1653 Stevens, J., Szombati, D., Maffei, M., Elouard, C., Assouly, R., Cottet, N., et al. (2022). Energetics of a
1654 single qubit gate. *Phys. Rev. Lett.* 129, 110601
- 1655 Stotland, A., Pomeransky, A. A., Bachmat, E., and Cohen, D. (2004). The information entropy of
1656 quantum-mechanical states. *Europhys. Lett.* 65, 700–706
- 1657 Szilard, L. (1929). On the reduction of entropy in a thermodynamic system by the interference of an
1658 intelligent being. *Zeit. Phys.* 53, 840–856
- 1659 Talkner, P., Lutz, E., and Hänggi, P. (2007). Fluctuation theorems: Work is not an observable. *Phys. Rev. E*
1660 75, 050102(R)
- 1661 Tindall, J., Fishman, M., Stoudenmire, E. M., and Sels, D. (2024). Efficient tensor network simulation of
1662 IBM's Eagle kicked Ising experiment. *PRX Quantum* 5, 10308
- 1663 Toffoli, T. (1982). Physics and computation. *Int. J. Theor. Phys.* 21, 165–175
- 1664 Toyabe, S., Sagawa, T., Ueda, M., Muneyuki, E., and Sano, M. (2010). Experimental demonstration of
1665 information-to-energy conversion and validation of the generalized Jarzynski equality. *Nature Phys.* 6,
1666 988–992
- 1667 Valavala, K. V., Coulson, K. D., Rajagopal, M. C., Gelda, D., and Sinha, S. (2018). Thermal engineering a
1668 the limits of the CMOS era. In *Handbook of Thin Film Deposition.*, eds. K. Seshan and D. Schepis (New
1669 York: Elsevier). 63–101
- 1670 Vallejo, A., Romanelli, A., and Donangelo, R. (2020). Out-of-equilibrium quantum thermodynamics in the
1671 Bloch sphere: Temperature and internal entropy production. *Phys. Rev. A* 101, 042132
- 1672 Vedral, V. (2002). The role of relative entropy in quantum information theory. *Rev. Mod. Phys.* 74, 197
- 1673 Verstraete, F., Audenaert, K., and Moor, B. D. (2001). Maximally entangled mixed states of two qubits.
1674 *Phys. Rev. A* 64, 012316
- 1675 Verstraete, F., Wolf, M. M., and Cirac, J. I. (2009). Quantum computation and quantum-state engineering
1676 driven by dissipation. *Nature Phys.* 5, 633
- 1677 Wallquist, M., Lantz, J., Shumeiko, V. S., and Wendin, G. (2005). Superconducting qubit network with
1678 controllable nearest-neighbour coupling. *New J. Phys.* 7, 178
- 1679 Wallraff, A., Schuster, D. I., Blais, A., Frunzio, L., Huang, R.-S., Majer, J., et al. (2004). Strong coupling of
1680 a single photon to a superconducting qubit using circuit quantum electrodynamics. *Nature* 431, 162–167

- 1681 Wang, G. M., Sevick, E. M., Mittag, E., Searles, D. J., and Evans, D. J. (2004). Experimental demonstration
1682 of violations of the Second Law of thermodynamics for small systems and short time scales. *Phys. Rev.*
1683 *Lett.* 89, 050601
- 1684 Wilce, A. (2021). Quantum Logic and Probability Theory. In *The Stanford Encyclopedia of Philosophy*,
1685 ed. E. N. Zalta (Metaphysics Research Lab, Stanford University). Fall 2021 edn.
- 1686 Wiltgen, A., Escobar, K. A., Reis, A. I., and Ribas, R. P. (2013). The computational complexity of linear
1687 optics. In *2013 26th Symposium on Integrated Circuits and Systems Design (SBCCI)*, eds. L. Fortnow
1688 and S. Vadhan (New York: IEEE), 1–6
- 1689 Wintersperger, K., Dommert, F., Ehmer, T., Hoursanov, A., Klepsch, J., Mauerer, W., et al. (2023). Neutral
1690 atom quantum computing hardware: performance and end-user perspective. *EPJ Quantum Tech.* 10, 32
- 1691 Wootters, W. K. (1998). Entanglement of formation of an arbitrary state of two qubits. *Phys. Rev. Lett.* 80,
1692 2245
- 1693 Wu, Y., Bao, W.-S., Cao, S., Chen, F., Chen, M.-C., Chen, X., et al. (2021). Strong quantum computational
1694 advantage using a superconducting quantum processor. *Phys. Rev. Lett.* 127, 180501
- 1695 Yamamoto, K., Duffield, S., Kikuchi, Y., and noz Ramo, D. M. (2024). Demonstrating Bayesian quantum
1696 phase estimation with quantum error detection. *Phys. Rev. Res.* 6, 013221
- 1697 Yamamoto, T., Pashkin, Y. A., Astafiev, O., Nakamura, Y., and Tsai, J. S. (2003). Demonstration of
1698 conditional gate operation using superconducting charge qubits. *Nature* 425, 941–944
- 1699 Yan, L. L., Xiong, T. P., Rehan, K., Zhou, F., Liang, D. F., Chen, L., et al. (2018). Single-atom
1700 demonstration of the Quantum Landauer Principle. *Phys. Rev. Lett.* 120, 210601
- 1701 Yang, J. F. and Shen, H. Z. (2024). Exceptional-point-engineered dispersive readout of a driven three-level
1702 atom weakly interacting with coupled cavities in non-Markovian environments. *Phys. Rev. A* 109,
1703 053712
- 1704 Yarkoni, S., Raponi, E., Back, T., and Schmitt, S. (2022). Quantum annealing for industry applications:
1705 introduction and review. *Rep. Prog. Phys.* 85, 104001
- 1706 You, J. Q., Hu, X., Ashhab, S., and Nori, F. (2007). Low-decoherence flux qubit. *Phys. Rev. B* 75, 140515
- 1707 Zhang, R., Chen, T., and Wang, X. B. (2017). Deterministic quantum controlled-PHASE gates based on
1708 non-Markovian environments. *New J. Phys.* 19, 123001
- 1709 Zhong, H.-S., Deng, Y.-H., Qin, J., Wang, H., Chen, M.-C., Peng, L.-C., et al. (2021). Phase-programmable
1710 gaussian boson sampling using stimulated squeezed light. *Phys. Rev. Lett.* 127, 180502
- 1711 Zhu, X., Saito, S., Kemp, A., Kakuyanagi, K., ichi Karimoto, S., Nakano, H., et al. (2011). Coherent
1712 coupling of a superconducting flux qubit to an electron spin ensemble in diamond. *Nature* 478, 221–224
- 1713 Zurek, W. H. (1982). Environment-induced superselection rules. *Phys. Rev. D* 26, 1862
- 1714 Zurek, W. H. (2003). Decoherence, einselection, and the quantum origins of the classical. *Rev. Mod. Phys.*
1715 75, 715–775
- 1716 Zwolak, M., Quan, H. T., and Zurek, W. H. (2009). Quantum Darwinism in a mixed environment. *Phys.*
1717 *Rev. Lett.* 103, 110402